Article (refereed)

Modelling the hydrological behaviour of a coffee agroforestry basin in Costa Rica

F. Gómez-Delgado[1,2], O. Roupsard[1,3], R. Moussa[4], M. van Oijen[5], P. Vaast[1], B. Rapidel[1,3], A. Pérez[3], J. M. Harmand[1], M. Voltz[4], G. le Maire[1], J. M. Bonnefond[6], P. Imbach[3] and S. Taugourdeau[1]

[1]{CIRAD, UPR80, Avenue d'Agropolis, 34398 Montpellier, France}

[2]{ICE, CENPE, 10032 San José, Costa Rica}

[3]{CATIE, 7170, 30501 Turrialba, Costa Rica}

[4]{INRA, UMR LISAH, 2 Place Viala, 34060 Montpellier, France}

[5]{CEH Edinburgh, Bush Estate, Penicuik EH26 0QB, United Kingdom}

[6]{INRA, EPHYSE, BP 81, 33883 Villenave d'Ornon, France}

Correspondence to: F. Gómez-Delgado (federico.gomez@cirad.fr)

Abstract

The profitability of hydropower in Costa Rica is affected by soil erosion and sedimentation in dam reservoirs, which are in turn influenced by land use, infiltration and aquifer interactions with surface water. In order to foster the provision and payment of Hydrological Environmental Services (HES), a quantitative assessment of the impact of specific land uses on the functioning of drainage-basins is required. The present paper aims to study the water balance partitioning in a volcanic coffee agroforestry micro-basin (1 km^2, steep slopes) in Costa Rica, as a first step towards evaluating sediment or contaminant loads. The main hydrological processes were monitored during one year, using flume, eddy-covariance flux tower, soil water profiles and piezometers. A new Hydro-SVAT lumped model is proposed, that balances SVAT (Soil Vegetation Atmosphere Transfer) and basin-reservoir routines. The purpose of such a coupling was to achieve a trade-off between the expected performance of ecophysiological and hydrological models, which are often employed separately and at different spatial scales, either the plot or the basin. The calibration of the model to perform

streamflow yielded a NS coefficient equal to 0.80, while the validation of the water balance partitioning was consistent with the independent measurements of actual evapotranspiration (R^2=0.79, energy balance closed independently), soil water content (R^2=0.49) and water table level (R^2=0.90). An uncertainty analysis showed that the streamflow modelling was precise for nearly every time step, while a sensitivity analysis revealed which parameters mostly affected model precision, depending on the season. It was observed that 64% of the incident rainfall R flowed out of the basin as streamflow, 25% as evapotranspiration and the remaining 11% was attributed to deep percolation. The model indicated an interception loss equal to 4% of R, a surface runoff of 5% and an infiltration component of 91%. The modelled streamflow was constituted by 63% of baseflow originating from the aquifer, 29% of subsurface non-saturated runoff and 8% of surface runoff. Given the low surface runoff observed under the current physical conditions (andisol) and management practices (no tillage, planted trees, bare soil kept by weeding), this agroforestry system on a volcanic soil demonstrated potential to provide valuable HES, such as a reduced superficial displacement-capacity for fertilizers, pesticides and sediments, as well as a streamflow regulation function provided by the highly efficient mechanisms of aquifer recharge and discharge. The proposed combination of experimentation and modelling across ecophysiological and hydrological approaches proved to be useful to account for the behaviour of a given basin, so that it can be applied to compare HES provision for different regions or management alternatives.

1 Introduction

The ability of ecosystems to infiltrate rainfall, sustain aquifers, and avoid erosion is a key determinant for the provision of hydrological environmental services (HES), especially in the humid tropics where surface fluxes can be very high (Millenium Ecosystem Assessment, 2005). Woody plants and in particular agroforestry (AF) systems associating shade trees and perennial crops with deep root systems are assumed to enhance these HES in comparison to traditional intensive cropping systems (Ataroff and Monasterio 1997; Vaast et al., 2005; Siles et al., 2010), but it is crucial to verify and quantify this hypothesis. Costa Rica is renowned as a promoter of HES by charging water users for the HES they receive from land owners (e.g. forest conservation), focusing on water quality (Pagiola, 2008). Hydropower producers, generating 78% of the total electricity consumption in Costa Rica during 2008 (ICE, 2009), are major HES payers. Coffee is one of the most traded agricultural commodities in the world

1   employing 100 million people (Vega and Rosenquist, 2001). In Costa Rica, coffee accounted

2   for 15% of the agricultural exports in 2008 and covered 2% of the territory (SEPSA, 2009).

3   As coffee plantations are present in the main basins used for hydroelectric generation in Costa

4   Rica, the eventual trade-offs of the payment of HES from hydropower producers to coffee

5   farmers become evident. Negotiation for these payments is facilitated between providers and

6   purchasers when the service, or the impact of a given practice on the provision of the service,

7   are clearly evaluated. However, links between land use, tree cover and hydrology in Costa

8   Rica have not been thoroughly investigated by quantitative research (Anderson et al., 2006).

9   There is a need of both, experimentation at the basin scale in order to evaluate the main

10   hydrological processes, and of integrated modelling to understand the behaviour of all water

11   compartments, including hidden ones (e.g. the aquifer).

12   The partitioning of the water balance (WB) is a pre-requisite to evaluate HES such as

13   infiltration, aquifer regulation capacity, erosion control and contaminants retention in coffee

14   AF systems. Comprehensive WB studies at basin scale, including closure verification by

15   independent methods, have been carried out in the developed world and for other land covers,

16   like those reported by Roberts and Harding (1996), Dawes et al. (1997), Ceballos and

17   Schnabel (1998), Wilson et al. (2001) and Maeda et al. (2006). Some experimental basins are

18   located in the tropics, like those in Brazil, Costa Rica, Guadeloupe and Panamá (Fujieda et al.,

19   1997; Genereux et al., 2005; Charlier et al., 2008; Kinner et al., 2004), but no coffee AF

20   basins have been equipped so far. Some reports are available for coffee AF systems but at the

21   plot level and for some particular fluxes such as throughfall and stemflow (Siles et al., in

22   rev.), tree and coffee transpiration (van Kanten and Vaast, 2006; Dauzat et al., 2001), surface

23   runoff (Harmand et al, 2007), energy balance and latent heat flux (Gutiérrez et al., 1994). To

24   our knowledge, there is no comprehensive study of the water balance partitioning of coffee

25   AF systems at the basin level, including the behaviour of the aquifer.

26   Truly balanced combinations of hydrological and ecophysiological experiments and models

27   remain scarce, although they intrinsically carry a more realistic and comprehensive

28   representation of plant, soil and aquifer components at plot and basin scales. Most

29   hydrological studies at basin scale use flumes for monitoring the streamflow and simply

30   estimate evapotranspiration (*ET*), which prevents a true verification of the water balance

31   closure or the estimation of deep percolation.

1   As in the tropics we assumed that *ET*, including the re-evaporation of intercepted water (R_{In}),

2   is an important component of the water balance, even for precipitations around 3000 mm

3   year^{-1}, we decided to measure it directly by eddy-covariance (Baldocchi and Meyers, 1998;

4   Wilson et al. 2001; Roupsard et al., 2006), choosing a 0.9 km^2 micro-basin embedded in a

5   very homogeneous coffee AF plantation. As an additional advantage, the eddy-covariance

6   method can be validated itself by closing the energy balance (Falge et al., 2001).

7   Lumped, conceptual rainfall-streamflow models have been used in hydrology since the 1960s

8   (e.g. Crawford and Linsley, 1966; Cormary and Guilbot, 1969; Duan et al., 1992; Bergström,

9   1995; Donigan et al., 1995; Havnø et al., 1995; Chahinian et al., 2005). These models

10   consider the basin as an undivided entity, and use lumped values of input variables and

11   parameters. For the most part (for a review, see Fleming, 1975; Singh, 1995), they have a

12   conceptual structure based on the interaction between storage compartments, representing the

13   different processes with mathematical functions to describe the fluxes between the

14   compartments. Most hydrological models simplify the *ET* component based on potential *ET*

15   routines (FAO, 1998) or using very empirical, non-validated models for actual *ET*. However,

16   improper parameterization of the crop coefficient may severely affect the parameterization of

17   hydrological resistances and fluxes. In constrast, ecophysiological models may operate

18   efficiently at plot level but miss the partitioning between lateral subsurface runoff and vertical

19   drainage, and the dynamics of water in aquifers and rivers. This is a major limitation for the

20   assessment of HES, which is mainly desired at the basin scale.

21   In the present study we attempted to couple two lumped models into a new and original

22   approach, chosen to be scalable and parsimonious: a basin reservoir model similar to the

23   CREC model (Cormary and Guilbot, 1969) and employing the Diskin and Nazimov (1995)

24   production function as proposed by Moussa et al. (2007a, 2007b), and the SVAT model

25   proposed by Granier et al. (1999). While the basin model was considered appropriate for its

26   simplicity and capacity to support new routines, the SVAT model was chosen for its

27   parsimony (three parameters in its basic formulation), its robustness (uses simple soil and

28   stand data in order to produce model runs for many years, avoiding hydraulic parameters that

29   are difficult to measure and scale up), its ability to quantify drought intensity and duration in

30   forest stands, and for its successful past validation in various forest stands and climatic

31   conditions, including tropical basins (Ruiz et al., 2010).

1   This paper aims to explain and model the hydrological behaviour of a coffee AF micro-basin

2   in Costa Rica, assessing its infiltration capacity on andisols. The methodology consists of

3   experimentation to assess the main water fluxes and modelling to reproduce the behaviour of

4   the basin. First, we present the study site and the experimental design. Second, we develop a

5   new lumped hydrological model with balanced ecophysiological/hydrological modules (that

6   we called Hydro-SVAT model). This model was tailored to the main hydrological processes

7   that we recorded (streamflow, evapotranspiration, water content in the non-saturated zone and

8   water table level) and that are described in the subsequent sections. Third, we propose a

9   multi-variable calibration/validation strategy for the Hydro-SVAT model so we calibrate

10   using the streamflow and validate using the remaining three variables. Fourth, we make an

11   uncertainty analysis to produce a confidence interval around our modelled streamflow values,

12   and a sensitivity analysis to assess from which parameters this uncertainty might come.

13   Finally, we discuss the main findings concerning the water balance in our experimental basin.

14

2   The study site

2.1   Location, climate and soil

17   The area of interest is located in Reventazón river basin, in the Central-Caribbean region of

18   Costa Rica (Fig. 1*a,b*). It lies on the slope of the Turrialba volcano (central volcanic mountain

19   range of the country) and drains to the Caribbean Sea. The Aquiares coffee farm is one of the

20   largest in Costa Rica (6.6 km^2), "Rainforest Alliance^{TM}" certified, 15 km from CATIE

21   (Centro Agronómico Tropical de Investigación y Enseñanza). Within the Aquiares farm, we

22   selected the Mejías creek micro-basin (Fig. 1c) for the "Coffee-Flux" experiment. The basin

23   is placed between the coordinates -83º44'39" and -83º43'35" (West longitude), and between

24   9º56'8" and 9º56'35" (North latitude) and is homogeneously planted with coffee (*Coffea*

25   *arabica* L., var Caturra) on bare soil, shaded by free-growing tall *Erythrina poeppigiana*

26   trees. The initial planting density for coffee was 6,300 plants ha^{-1}, with a current age >30

27   years, 20% canopy openness and 2.5 m canopy height. It is intensively managed and

28   selectively pruned (20% per year, around March). Shade trees have a density of 12.8 trees ha^{-1},

29   with 12.3% canopy cover and 20 m canopy height. The experimental basin has an area of

30   0.9 km^2, an elevation range from 1,020 up to 1,280 m.a.s.l. and a mean slope of 20%.

1   Permanent streams extend along 5.6 km, implying a drainage density of 6.2 km km^{-2}. The

2   average slope of the main stream is 11%.

3   According to the classification by Mora-Chinchilla (2000), the experimental basin is located

4   along a 1.3 km wide strip of volcanic avalanche deposits, characterized by chaotic deposits of

5   blocks immersed in a matrix of medium-to-coarse sand, which is the product of the collapse

6   of the south-eastern slope of Turrialba volcano's ancient crater. The general classification

7   given by the geological map of Costa Rica (MINAE-RECOPE, 1991) describes the general

8   stratigraphy as shallow intrusive volcanic rocks, and the particular region as proximal facies

9   of modern volcanic rocks (Quaternary), with presence of lava flows, agglomerates, lahars and

10 ashes. Soils belong to the order of andisols according to the USDA soil taxonomy, which are

11 soils developing from volcanic ejecta, under weathering and mineral transformation

12 processes, very stable, with high organic matter content and biological activity and very large

13 infiltration capacities.

14 According to Köppen-Geiger classification (Peel et al. 2007), the climate is tropical humid

15 with no dry season and strongly influenced by the climatic conditions in the Caribbean

16 hillside. The mean annual rainfall in the study region for the period 1973-2009 was estimated

17 as 3014 mm at the Aquiares farm station (Fig. 2). At the experimental basin the rainfall in

18 2009 (3208 mm) was close to the annual mean, but showed a monthly deviation of ±100 mm

19 around the historical regime. Mean monthly net radiation ranged in 2009 from 5.7 to 13.0 MJ

20 m^{-2} d^{-1}, air temperature from 17.0 to 20.8 °C, relative humidity from 83 to 91 %, windspeed at

21 2 m high from 0.4 to 1.6 m s^{-1} and potential evapotranspiration (FAO, 1998) from 1.7 to 3.8

22 mm d^{-1}.

23 **2.2 Experimental setup**

24 The "Coffee-Flux" experimental basin and instrument layout was designed to trace the main

25 water balance components employing spatially representative methods (Fig. 1*c*). It is part of

26 the FLUXNET network for the monitoring of greenhouse gases of terrestrial ecosystems. The

27 hydrological measurements were recorded from December 2008 up to February 2010.

28 Rainfall and climate: rainfall was monitored at 3 m above ground in the middle of 3 transects

29 of the basin, using three lab-intercalibrated ARG100 tipping-bucket (R.M. Young, MI, USA)

30 connected to CR800 dataloggers (Campbell Scientific, Shepshed, UK), and integrated every

31 10 min. Other climate variables were logged on top of the eddy-flux tower with a CR1000,

1   every 30 s, integrated half-hourly and using: Net radiation: NR-Lite (Kipp & Zonen, Delft,

2   The Netherlands); PPFD: Sunshine sensor BF3 (Delta-T devices Ltd, U.K.); temperature and

3   humidity: HMP45C in URS1 shelter (Campbell Scientific); wind-speed and direction: 03001

4   Wind Sentry (R.M. Young, MI, USA). The theoretical evapotranspiration from a wet grass

5   placed under local climate conditions, ET_0, was computed in accordance with FAO (1998).

6   Streamflow: a long-throated steel flume (length: 3.9 m; width: 2.8 m; height: 1.2 m) was

7   home-built to measure the streamflow at the outlet of the experimental basin, to record up to 3

8   m^3 s^{-1}, the maximum estimated discharge for the study period from an intensity-duration-

9   frequency analysis. The flume was equipped with a PDCR-1830 pressure transducer

10   (Campbell Scientific) to record water head at gauge point (30 s, 10 minutes integration), while

11   the rating curve was calculated considering the geometric and hydraulic properties of the

12   flume using Winflume software (Wahl et al., 2000). A validation of the rating curve was

13   made successfully using the salt dilution method as well as a pygmy current meter.

14   Soil water content: a frequency-domain-reflectometry portable probe (FDR Diviner2000,

15   Sentek Pty Ltd) was used to survey 20 access tubes distributed in the three study transects to

16   provide the mean volumetric soil water in the basin. The sensor measures at 10 cm intervals,

17   reaching a total depth of 1.6 m. A measurement campaign through the 20 sites was carried out

18   every week. The sensors were calibrated by digging sampling pits in the vicinity of six test

19   tubes, to obtain the actual volumetric soil water content from gravimetric content and dry bulk

20   density.

21   Evapotranspiration: the actual evapotranspiration from the soil, coffee plants and shade trees

22   was measured at reference height (26 m) on the eddy-covariance tower, similarly to Roupsard

23   et al. (2006). 3D wind components and temperature were measured with a WindMaster sonic

24   anemometer (Gill Instruments, Lymington, UK) at 20 Hz. H_2O fluctuations were measured

25   with a Li-7500 open path (LiCor, Lincoln, NE, USA). Raw data were collected and pre-

26   processed by "Tourbillon" software (INRA-EPHYSE, Bordeaux, France) for a time-

27   integration period of 300 s, then post-processed using EdiRe software (University of

28   Edinburgh, UK) into half-hourly values and quality checked. A validation was made by direct

29   comparison of the measured net radiation R_n with the sum of sensible heat flux (H) and latent

30   heat flux (λE): at daily time step, this yielded $H+\lambda E=0.92$ R_n (R^2 = 0.93) which was

31   considered sufficiently accurate to assume that advection effects on λE could be neglected

32   here. Due to lighting and sensor breakdown, 45 days of data were lost between July and

1   August 2009. To gap-fill the missing period we used the Penman-Monteith model, whose

2   canopy conductance was adjusted using measured values.

3   Leaf Area Index (*LAI*): the coffee light transmittance was measured monthly in diffuse light

4   conditions, for five rings at different zenital angles (LAI2000, Li-COR Corvallis, USA), along

5   three 50 m-long transects through the flux tower plot, similarly to Roupsard et al. (2008).

6   Effective coffee *LAI*, obtained from this light transmittance, was converted into actual *LAI*

7   according to Nilson (1971), using a ratio of effective to actual *LAI* that was estimated from a

8   dedicated calibration. The actual coffee *LAI* was measured directly on a small plot by

9   counting total leaf number of 25 coffee plants, measuring leaf length and width every 20

10 leaves and using empirical relationships between leaf length and width and leaf area (LI-

11 3100C, Li-COR) ($R^2 > 0.95$). On the same small plot, the effective *LAI* was measured with

12 LAI2000. The ratio of effective to actual *LAI* was then calculated on this small plot (1.75) and

13 was considered to be constant with time and space in the micro-basin, allowing the estimation

14 of the actual *LAI* on the three LAI2000 transects. The *LAI* for shade trees was estimated using

15 their crown cover projection (on average 12.3% over the whole basin) observed on a very

16 high resolution panchromatic satellite image (WorldView image, February 2008, 0.5 m

17 resolution). As we did not have measurements of *LAI* for shade trees, we considered this *LAI*

18 in the order of magnitude of coffee *LAI* on a crown-projected basis, and therefore we

19 multiplied the actual coffee *LAI* measured on transects by 1.123, to estimate the ecosystem

20 *LAI* (tree and coffee). In order to monitor the time-course of ecosystem *LAI* at the basin scale,

21 we combined these ground measurements with time series of remotely-sensed images. We

22 used time series of Normalized Difference Vegetation Index (NDVI) from Moderate

23 Resolution Imaging Spectroradiometer (MODIS) data products MOD13Q1 and MYD13Q1

24 (16-Day composite data, 250m resolution). NDVI is known to be correlated with the green

25 *LAI* if it is low, for most ecosystems (Rouse et al., 1974). Twenty-three MODIS pixels

26 covering the experimental basin were selected, and their NDVI time series were downloaded.

27 We filtered the raw NDVI time series according to quality criterion given in the MODIS

28 products, and we adjusted a smooth spline function on it as in Marsden et al. (2010). Then, a

29 linear regression between the smoothed NDVI of the pixel including the flux tower and

30 ground values of actual ecosystem *LAI* was calibrated ($R^2 = 0.69$). This regression was used

31 on other pixels of the basin, and averaged to have the annual time-course of actual *LAI*.

1 Water table level: four piezometric wells measuring up to 4 m depth were built in the three

2 main transects of study. They were equipped with pressure transducers (Mini-Divers,

3 Schlumberger Water Services) that measure and record the water table level every 30

4 minutes.

5 Period of measurement, data gaps and gap-filling: the recording information is given in Table

6 1 for the five hydrologic variables. The frequency of measurement varies, but is finally

7 calculated at the 30 minutes time step (except for soil water content that is a non-continuous

8 measurement). When gaps are present in the measurements, a gap filling method was applied.

9

3   Hydro-SVAT lumped model

11 We designed a lumped, five-reservoir-layer model to predict the water balance (WB)

12 partitioning (stocks and fluxes) at the scale of the whole basin. It is based on the water

13 balance models developed by Moussa et al. (2007a, 2007b) and Granier et al. (1999), and

14 built to reproduce the main hydrological processes measured at the experimental basin, which

15 will be presented in Sect. 4. The model of Moussa et al. (2007a, 2007b) works at the basin

16 scale and simulates the ecosystem evapotranspiration rather roughly, while the one of Granier

17 et al. (1999) works at the plot scale and totally ignores the lateral water fluxes through the soil

18 and the role of the basin aquifers. The main novelties of the Hydro-SVAT model with respect

19 to the model structure of Moussa et al. (2007a, 2007b) are the inclusion of a land cover

20 reservoir to separate the intercepted rainfall from the combined throughfall/stemflow

21 component, and the partition of non-saturated soil into two reservoirs, one with and one

22 without roots of plants and trees. The first of these innovations intends to take into account

23 the non-negligible interception loss in coffee AF systems, as reported by Jiménez (1986),

24 Harmand et al. (2007) and Siles (2007). The second innovative addition to the model is to

25 better represent the water dynamics in the non-saturated soil, given that only its upper layer

26 will lose humidity by root extraction. The water balance model of Granier et al. (1999) is

27 incorporated in this superficial reservoir but in a simplified form, so that both, the root

28 distribution and the soil porosity, are homogeneous through the vertical, non-saturated profile.

29 Hence, the water content in this reservoir is the variable linking our two parent models.

30 The modelling hypotheses governing the model architecture were: a) the interception loss

31 component is not negligible in the WB and is a function of rainfall intensity, b) infiltration is a

32 function of the soil water content in the non-saturated reservoirs, c) evapotranspiration is a

9

1   significant component in the WB and is best described using a SVAT model that couples

2   evapotranspiration to root water extraction from the soil, d) the aquifer has a higher discharge

3   rate above a threshold level, and e) there is a net water outflow from the system as deep

4   percolation.

5   The model was implemented using Matlab® V. R2007a (The MathWorks Inc., USA).

6   3.1   Model structure

7   The model structure is presented in Fig. 3. The next three sections will describe the model

8   structure according to its three major routines and five layers. The first layer is called "land

9   cover reservoir" and separates the total rainfall into an intercepted loss and a joint

10   throughfall/stemflow component. The second layer or "surface reservoir" regulates the

11   surface runoff. The infiltration process from the second layer is controlled by the joint water

12   content at the third and fourth layers, called "non-saturated root reservoir" and "non-saturated

13   non-root reservoir", respectively. The evapotranspiration flux is calculated at the "non-

14   saturated root reservoir", while both non-saturated layers control the drainage, the percolation

15   and the non-saturated runoff processes. The fifth and last layer is the "aquifer reservoir",

16   which determines the baseflow and the deep percolation. Finally, we will explain the sum of

17   the total runoff and baseflow components and the routing procedure to generate the modelled

18   streamflow. Let $A(t)$, $B(t)$, $C(t)$, $D(t)$ and $E(t)$ [L] be the water levels at time t in the five

19   reservoirs A, B, C, D and E, respectively (or land cover reservoir, surface reservoir, non

20   saturated root reservoir, non-saturated no-root reservoir and aquifer reservoir). Let A_X, B_X, C_X,

21   D_X and E_X [L] be the water levels corresponding to the maximum holding capacities for the

22   five reservoirs.

23   3.1.1 Infiltration and actual evapotranspiration

24   a. Infiltration

25   The infiltration process i [LT^{-1}] occurs from the second layer (surface reservoir) to the third

26   one (non-saturated root reservoir), and eventually to the fourth one (non-saturated non-root

27   reservoir) when i fills the third one. The infiltration capacity $f_i(t)$ [LT^{-1}] is a state variable that

28   depends on the joint water level in these non-saturated reservoirs, given by the conceptual

29   state variable $CD(t) = C(t) + D(t)$ [L]. Similarly, we define $CD_X = C_X + D_X$ [L] and $CD_F = C_F$

30   $+ D_F$ [L] as the conceptual joint water levels for maximum and field holding capacities,

1 respectively, in the two coupled non-saturated soil reservoirs. Then, $f_i(t)$ is calculated as (see

2 Fig. 4*a*):

3 If $CD(t) < CD_F$ then $f_i(t) = f_0 + (f_c - f_0) CD(t) CD_F^{-1}$ (1)

4 If $CD(t) \geq CD_F$ then $f_i(t) = f_c$ (2)

5 where f_0 [LT^{-1}] is the maximum infiltration capacity ($f_0 = \alpha\, f_c$) and f_c [LT^{-1}] is the

6 infiltration rate at field capacity. The infiltration i both modifies and depends on $B'(t)$,

7 is the water availability in the second reservoir before i is extracted, according to: which

8 If $B'(t) \Delta t^{-1} < f_i(t)$ then $i = B'(t) \Delta t^{-1}$ and $B(t) = 0$ (3)

9 If $B'(t) \Delta t^{-1} \geq f_i(t)$ then $i = f_i(t)$ and $B(t) = B'(t) - f_i(t)$ (4)

10 The infiltration module calculates the infiltration i as output variable, using the state variables

11 $B(t)$, $C(t)$, $D(t)$ and $f_i(t)$. Six parameters (C_X, D_X, C_F, D_F, f_c and α) are demanded.

12 **b. Evapotranspiration**

13 The evapotranspiration component ET [LT^{-1}] acts directly on the third layer (non-saturated

14 root reservoir) and is the sum of E_u [LT^{-1}] the understory and soil evaporation, and of T [LT^{-1}]

15 the transpirational water uptake by roots.

16 $ET = E_u + T$ (5)

17 According to Shuttleworth and Wallace (1985), the fraction of total evapotranspiration

18 originating from the plants is close to 100% of the total evapo-transpiration of the ecosystem

19 when *LAI* >3 an when the soil is not saturated at its surface, which was always the case in our

20 study. We thus assumed for simplicity that E_u, the evaporation from the soil, was nil.

21 Transpiration T is obtained by solving T from the lightly modified ratio: $r = T\, ET_0^{-1}$

22 [dimensionless] proposed by Granier et al. (1999). We substituted the original Penman

23 potential evapotranspiration *PET* in that ratio by the Penman-Monteith potential

24 evapotranspiration ET_0 [LT^{-1}] (FAO, 1998). While ET_0 was calculated at each time step Δt,

25 we estimated r as a function of the relative extractable water *REW(t)* [dimensionless], a state

26 variable given by Granier et al. (1999) as:

27     $REW(t) = C(t)\,C_F^{-1}$ (6)

1   The $REW(t)$ is linked to the soil water content according to:

2     $$REW(t) = \frac{\theta(t) - \theta_r}{\theta_f - \theta_r} \qquad (7)$$

3   with $\theta(t)$: volumetric soil water content [$L^3 L^{-3}$] at time t θ_r: residual soil water content [$L^3 L^{-3}$]

4   and θ_f: soil water content at field capacity [$L^3 L^{-3}$].

5   The parameter REW_c [dimensionless] is the critical $REW(t)$ below which the transpiration of

6   the system begins to decrease. Figure 4b shows an example of some r curves as a function of

7     $REW(t)$. Each curve can be defined only by REW_c and the rm_{LAI}, a maximum value for the

8   ratio r that depends on the LAI of the system as:

9     $$rm_{LAI} = LAI \; LAI_X^{-1} \; r_m \qquad (8)$$

10   where LAI_X is the maximum measured LAI during the modelling period and r_m is a parameter

11   indicating the maximum ratio $T \, ET_0^{-1}$ that can be found in this system. Then:

12   If $REW(t) < REW_c$ then $r = rm_{LAI} \; REW(t) \, REW_c^{-1}$ (9)

13   If $REW(t) \geq REW_c$ then $r = rm_{LAI}$ (10)

14   Finally, we find the transpiration as $T = r \, ET_0$. The total modelled evapotranspiration

15   including the interception loss, can be calculated as: $ETR_m = E_u + T + R_{In}$, with R_{In} [LT^{-1}]

16   being the intercepted/evaporated rainfall loss that will be explained in the next section. Hence,

17   ETR_m can be directly compared to the evapotranspiration that we measured at the flux tower.

18   This module provides the evapotranspiration ET as a function of the state variable $C(t)$, two

19   input variables (LAI and ET_0) and three parameters (C_X, REW_c and r_m).

20   ### 3.1.2 Water balance in the model reservoirs

21   **a. Land cover reservoir**

22   The first layer of the model, denoted "land cover reservoir", represents the soil cover in the

23   basin and controls the partition of the total incident rainfall R [LT^{-1}] in intercepted (then

24   evaporated) rainfall loss R_{In} [LT^{-1}] and the combined troughfall/stemflow R_{TS} [LT^{-1}]. A simple

25   water balance of this reservoir is established to calculate a proxy $A'(t$ [L] of the final water
)

26   level $A(t)$ for each time step t, by adding the incident rainfall R and subtracting the Penman

27   potential evapotranspiration PET [LT^{-1}] from the existing land cover humidity level $A(t-1)$:

1    $A'(t) = A(t-1) + R - PET$ (11)

2   We calculated the water level $A(t)$ in this reservoir as well as R_{TS} and R_{In} by differentiating

3   three cases:

If $A'(t) \leq 0$ then $A(t) = 0$ and $R_{In} = A(t-1) + R$ and $R_{TS} = 0$ (12)

If $0 < A'(t) < A_X$ then $A(t) = A'(t)$ $R_{In} = PET$ and   and $R_{TS} = 0$ (13)

If $A'(t) \geq A_X$ then $A(t) = A_X$ and $R_{In} = PET$ and $R_{TS} = A'(t) - A_X$ (14)

4   The land cover module calculates at each time t the water level $A(t)$ as a state variable,

5   demanding two input variables (R and PET) and one parameter (A_X). It yields the partition of

6   R into R_{In} and R_{TS}.

7   **b. Surface reservoir**

8   The second layer is called "surface reservoir" and acts as a sheet top soil with a given

9   roughness and surface runoff delaying properties. The water balance in this surface reservoir

10   for a given interval Δt is:

11    $B(t) = B(t-1) + R_{TS} - Q_{B1} - Q_{B2} - i$ (15)

12   where R_{TS} [LT^{-1}] is the combined throughfall/stemflow component from the previous layer

13   and Q_{B1} and Q_{B2} [LT^{-1}] are the non-immediate and immediate surface runoffs calculated as:

14    $Q_{B1} = k_B B(t)$ (16)

15   where k_B [T^{-1}] is a discharge parameter, and:

16   If $B(t) \leq B_X$ then $Q_{B2} = 0$ (17)

17   If $B(t) > B_X$ then $Q_{B2} = [B(t) - B_X] \Delta t^{-1}$ (18)

18   If $Q_{B2} > 0$ then the water level $B(t)$ is reset to B_X. The infiltration i [LT^{-1}] is a function of the

19   coupled water content in the third and the fourth layers and is the last component to be

20   evaluated in the surface reservoir.

21   This surface reservoir module calculates the water level $B(t)$ as a state variable and demands

22   one input variable (R_{TS}), and two parameters for the reservoir (B_X and k_B). It produces three

23   output variables: i, Q_{B1} and Q_{B2}. The two latter variables constitute the surface runoff in the

24   basin (Fig. 4*c*).

1   **c. Non-saturated root reservoir**

2   The "non-saturated root reservoir" is the third layer of the model and it represents a soil layer

3   with presence of root systems from trees and plants. The water balance here is:

4   $C(t) = C(t-1) + i - ET - d_1 - d_2 -$ (19)

Q_C

5   where $C(t)$ [L] is the state variable of the water level at a given time t, i is the infiltration from

6   the second layer, ET [LT^{-1}] is the evapotranspiration, d_1 and d_2 [LT^{-1}] are the non-immediate

7   and immediate drainages to the fourth layer, respectively and Q_C [LT^{-1}] is the non-saturated

8   runoff from the root reservoir.

9   There will be immediate drainage d_2 if at anytime the R_{TS} component fills the reservoir above

10 C_X. Then $d_2 = [C(t) - C_X] \Delta t^{-1}$ goes to the fourth layer and $C(t)$ is reset to C_X. Both non-

11 immediate drainage d_1 and non-saturated runoff Q_C occur whenever $C(t)$ is higher than the

12 field capacity threshold C_F [L] according to:

13 $\rho = [C(t) - C_F]$ (20)

k_C

14 where ρ [LT^{-1}] is the total outflow capacity in this reservoir and k_C [T^{-1}] a discharge

15 parameter. The partition of ρ in d_1 and Q_C depends on a parameter β [dimensionless], with $0 <$

16 $\beta < 1$. Then:

17 $d_1 = (1 - \beta)$ and $Q_C = \beta$ (21)

ρ ρ

18 The root soil module calculates the water level $C(t)$ as state variable using two input variables

19 (i and ET) and four parameters (C_X, C_F, k_C and β). It provides three outputs (d_1, d_2 and Q_C).

20 **d. Non-saturated non-root reservoir**

21 The fourth layer of the model is denoted "non-saturated non-root reservoir" and represents a

22 soil layer with total absence of root systems and hence, of root water extraction. The water

23 balance here is given by:

24 $D(t) = D(t-1) + d_1 + d_2 - Q_D - g_1 - g$ (22)

2

25 where $D(t)$ [L] is the state variable of the water level at a given time t, d_1 and d_2 [LT^{-1}] are the

17

26 non-immediate and immediate drainages from the third layer, respectively; Q_D [LT^{-1}] is the

27 non-saturated runoff from the non-root reservoir and g_2 and g_1 [LT^{-1}] are the immediate and

28 non-immediate percolation to the fifth model layer, respectively.

1   Immediate percolation g_2 will be produced if at anytime the drainage (d_2 and/or d_1) fills the

2   reservoir above D_X. Then $g_2 = \left[D(t) - D_X\right]\Delta t^{-1}$ moves to the aquifer reservoir and $D(t)$ is

3   reset to D_X. Both non-immediate percolation g_1 and non-saturated runoff Q_D occur whenever

4   $D(t)$ is higher than the field capacity threshold D_F [L]:

5   $$\eta = \left[D(t) - D_F\right]k_D \qquad (23)$$

6   where η [LT^{-1}] is the total outflow capacity of this reservoir and k_D [T^{-1}] a discharge

7   parameter. The partition of η in g_1 and Q_D depends on the parameter β [dimensionless]. Then:

8   $$\frac{g_1}{\eta} = (1 - \beta) \quad \text{and} \quad \frac{Q_D}{\eta} = \beta \qquad (24)$$

9   The non-root soil module calculates the water level $D(t)$ as state variable using two input

10 variables (d_1 and d_2) and four parameters (D_X, D_F, k_D and β). It provides three outputs (g_1, g_2

11 and Q_D).

e. Aquifer reservoir

13 A fifth layer called "aquifer reservoir" represents the groundwater system and controls

14 baseflow and deep percolation. The reservoir is composed by a shallow aquifer that acts

15 whenever the water level in the reservoir is higher than E_X, and by a deep aquifer with a

16 permanent contribution. The water balance here is:

17 $$E(t) = E(t-1) + g_1 + g_2 - Q_{E1} - Q_{E2} - DP \qquad (25)$$

18 where $E(t)$ [L] is the state variable of the water level at a given time t, g_1 and g_2 [LT^{-1}] are

19 respectively the non-immediate and immediate percolation from the fourth layer, Q_{E1} and Q_{E2}

20 [LT^{-1}] are the baseflow from deep and shallow aquifers respectively (Fig. 4d), and DP [LT^{-1}]

21 is the deep percolation.

22 If $E(t) \leq E_X$ then $Q_{E1} = k_{E1}E(t)$ and $Q_{E2} = 0$ $\qquad$ (26)

23 If $E(t) > E_X$ then $Q_{E1} = k_{E1}E_X$ and $Q_{E2} = k_{E2}\left[E(t) - E_X\right]$ $\qquad$ (27)

24 $DP = k_{E3}E(t)$ $\qquad$ (28)

25 where k_{E1}, k_{E2}, and k_{E3} are discharge parameters controlling deep/shallow aquifers and deep

26 percolation, respectively.

15

27   This module calculates the water level $E(t)$ as state variable using two input variables (g_2 and

28   g_1) and four parameters (E_X, k_{E1}, k_{E2} and k_{E3}), to provide three outputs (Q_{E1}, Q_{E2} and DP).

3.1.3 Total runoff, baseflow and streamflow

The components of surface runoff, non-saturated runoff and baseflow are added to obtain the total runoff Q_T [LT^{-1}]:

$$Q_T = Q_B + Q_C + Q_D + Q_E \qquad (29)$$

As explained in Moussa and Chahinian (2009) the streamflow Q [LT^{-1}] at the outlet of the basin is obtained by the routing of Q_T using a transfer function (to take into account the water travel time). The Hayami (1951) kernel function (an approximation of the diffusive wave equation) is developed to obtain a unit hydrograph linear model for this purpose. That is:

$$Q(t) = \int_0^t Q_T(\tau)\, H(t - \tau)\, d\tau \qquad (30)$$

$H(t)$ is the Hayami kernel function, equal to:

$$H(t) = \left(\frac{w\, z_F}{\Pi}\right)^{\frac{1}{2}} \frac{e^{\, z_F \left(2 - \frac{t}{w} - \frac{w}{t}\right)}}{t^{3/2}} \quad \text{and} \quad \int_0^\infty H(t)\, dt = 1 \qquad (31)$$

where w [T] is a time parameter that represents the centre of gravity of the unit hydrograph (or the travel time) and z_F [dimensionless] a form parameter. Q in [LT^{-1}] units can be transformed to volume units [L^{3}T^{-1}] multiplying it by the basin area [L^2].

3.2 Model parameterization, calibration and validation

Summarizing, this Hydro-SVAT model uses four input variables: rainfall R, Penman-Monteith ET_0, Penman PET and leaf area index LAI to generate five main output variables: interception R_{In}, infiltration i, evapotranspiration ET, discharge components $Q = Q_B + Q_C + Q_D + Q_E$ (from surface, non-saturated and aquifer reservoirs, respectively) and deep percolation DP.

Five state variables are calculated for every time step, the water levels in the five reservoirs: $A(t)$, $B(t)$, $C(t)$, $D(t)$ and $E(t)$. $C(t)$ and $D(t)$ are summed to calculate $CD(t)$ an equivalent water content for the non-saturated reservoirs, producing a coupled discharge Q_{CD}.

In our experimental basin we applied the model for a one-year period (2009), a time step $\Delta t = 30$ minutes (1800 s) and a basin area equal to 0.886 km^2.

1   This model contains 20 parameters that are used to calculate infiltration (C_X, D_X, C_F, D_F, fc

2   and α), evapotranspiration (REW_c and r_m), the exchange between reservoirs (A_X, B_X, k_B, k_C, k_D,

3   β, E_X, k_{E1}, k_{E2} and k_{E3}) and the basin transfer function (w and z_F).

4   Four out of these 20 parameters (C_X, D_X, C_F, D_F) were estimated using field data. For

5   instance, two excavation experiments down to 3.5 m showed that very few roots were present

6   below 1.5 m, where the andisol layer turns into a more clayey, compact and stony deposit.

7   Then, the depth of the non-saturated root soil layer was fixed at $C_H = 1.6$ m (for simplicity,

8   equal to the length of our FDR probe tubes). The depth of the non-root layer was estimated in

9    $D_H = 1.0$ m. Following the relationships $C_X = (\theta_s - \theta_r) C_H$ and $D_X = (\theta_s - \theta_r) D_H$, the levels

10   for maximum water holding capacities in the non-saturated reservoirs can be calculated, as

11   well as the levels for field capacities, using the equations $C_F = (\theta_f - \theta_r) C_H$ and

12   $D_F = (\theta_f - \theta_r) D_H$. The volumetric soil water contents θ were estimated as $\theta_r = 0.37$: the

13   residual water content equal to the minimum θ observed in the basin during the study period;

14   $\theta_s = 0.63$: the θ at saturation for a typical andisol, according to Hodnett and Tomasella (2002);

15   and $\theta_f = 0.43$: the θ at field capacity equal to the average van Genuchten value for a matric

16   potential $= -10$ kPa (Hodnett and Tomasella, 2002).

17   Three parameters were taken from literature reviews and expert criteria (A_X, REW_c and r_m).

18   We set the surface reservoir maximum storage capacity A_X for our coffee AF system equal to

19   4×10^{-4} m using data from Siles et al. (in rev.). The two parameters of the evapotranspiration

20   routine were taken as: $REW_c = 0.4$ from Granier et al. (1999) and $r_m = 0.8$ from field

21   measurements of $T\,ET_0^{-1}$ (data not shown).

22   One parameter (B_X) was obtained at the end of the optimization process in order to fit the

23   maximum observed streamflow peak (this parameter is very sensitive as it acts directly on the

24   highest peaks). Two other parameters (w and z_F) were separately estimated by a trial and error

25   procedure, given the low sensitivity of the model to their variation.

26   The remaining 10 empirical parameters (fc, α, k_B, k_C, k_D, β, E_X, k_{E1}, k_{E2} and k_{E3}) were

27   simultaneously optimized. For this purpose we used the Nelder-Mead simplex algorithm

28   included in Matlab on 17520 semi-hourly time steps (one year). Convergence was reached

29   within 1000 runs and the stabilization of all parameter values by the end of the iteration

30   process was checked. A two-step calibration procedure was applied: a) selection of an initial

31   value for each parameter, falling within the respective range (fourth column, Table 2), and b)

1 simultaneous estimation of parameter values that maximize an objective function (sixth

2 column, Table 2), in this case the Nash and Sutcliffe (1970) efficiency coefficient.

3 Considering that we have only one year of measurements at hand, the presence of seasonality

4 in the data makes inadequate the use of partial validation methods (such as split-sample or

5 bootstrapping), so we calibrated the model using only the streamflow Q, and then validated it

6 using the remaining three measured variables: evapotranspiration ETR, water content in the

7 non-saturated zone θ and water table level z. For ETR we grouped the measured and modelled

8 values (given in the same units) at the daily time scale, which is the original time scale in

9 Granier's model, and then we excluded the gap-filled values. To calculate the modelled θ

10 from the water level in the root reservoir $C(t)$ we used the relation

11 $\theta = C(t)\,C_X^{-1}\left(\theta_s - \theta_r\right) + \theta_r$, while the observed values were obtained as the average of the

20

12 FDR point-measurements throughout the basin. To validate z we proposed an effective

13 porosity of the aquifer $n_A = 0.39$, to be able to directly link piezometric measurements z with

14 the modelled water level in our aquifer reservoir $E(t)$, according to $z = E(t)/n_A$.

15 Finally, we performed an analysis of model residuals: zero expectancy, normality,

16 homoscedasticity and standardized residuals.

17 **3.3   Uncertainty and sensitivity analysis**

18 In order to investigate the uncertainty in model predictions we performed a Monte-Carlo

19 approach on a restricted subset of parameter combinations, as suggested by Helton (1999).

20 For each of the 10 parameters a range was created with a deviation of ±30% around the

21 optimum value found in the calibration process, following the "one-at-a-time" method

22 described by Hamby (1995). Then, we assumed a uniform distribution, using the Latin

23 Hypercube function of Simlab 2.2 (http://simlab.jrc.ec.europa.eu) in order to produce a

24 sample from a joint probability distribution, ten times the number of parameters as

25 recommended, i.e. 100 parameter combinations. These combinations were introduced into the

26 calibrated Matlab program and we retrieved 100 output results of streamflow for each of the

27 17520 semi-hourly time steps. Instead of generating 17520 empirical confidence intervals

28 using the respective frequency distributions, we preferred to build confidence intervals around

29 the modelled streamflow at each time step, by assuming a given probability distribution and

30 estimating its parameters. First we proposed the normal distribution and checked 1% of the

18

31   time steps (175 distributions), most of which corresponded to recession phases: 146 out of

these 175 distributions (83%) presented a large asymptotic-significance value (>0.05) in a Kolmogorov-Smirnov test so they resembled normal distributions. However, after sampling another set of 1% time steps in the highest streamflow values (peaks), only 43% of them were normally distributed. Therefore we could not assume normality for our data set and we used Chebyshev's inequality to calculate more generic and conservative 95% and 99% confidence intervals.

The sensitivity analysis (SA) was also carried out using Simlab to determine which of the input variables contributed significantly to this modelling uncertainty. Two separate assessments were produced. First, a summary (through the time) index for model performance was studied: the Nash-Sutcliffe coefficient NS, being assessed by four sensitivity indexes: Pearson, Spearman, standardized regression and standardized rank regression coefficients (Hamby, 1994, 1995). Then, a second approach of sensitivity analysis was tested to try to follow the behaviour of the Spearman coefficient for each of the 10 parameters included in the SA through all time steps, as in Helton (1999).

The sensitivity indexes are calculated departing from the joint probability sample matrix x_{ij} of size $m \times n$, where m is the sample size and n the number of independent variables (here our 10 parameters) to study. The Monte Carlo evaluation of x_{ij} in the model will produce the result vector y_i, configuring the matrix system $[y_i : x_{ij}]$. Then, the Pearson product moment correlation (PEAR) for a given parameter j is the linear correlation coefficient between the variables x_{ij} and y_i across the m samples. To account for non-linear relationships that can be hidden by indicators like PEAR, a simple rank transformation is applied, replacing the original x-y series with their corresponding ranks $R(x)$ and $R(y)$. Then, the Spearman coefficient (SPEA) is obtained by calculating the correlation on the transformed data, as $SPEA(x, y) = PEAR[R(x), R(y)]$. The standardized regression coefficients (SRC) are the result of a linear regression analysis performed on $[y_i : x_{ij}]$ but previously standardizing all the variables. This is useful to evaluate the effect of the independent variables on the dependent one, without regarding their units of measurement, and can be computed by standard statistical methods. Finally, the standardized rank regression coefficients are obtained as $SRRC(x, y) = SRC[R(x), R(y)]$.

4   Results

In the 0.9 km^2 micro-basin of Mejías creek, within the Cafetalera Aquiares AF coffee farm, we obtained one full year (2009) of comprehensive experimental results of streamflow, evapotranspiration, soil water content and piezometry that we used to calibrate and validate the Hydro-SVAT model. First we present the hydrological behaviour of the basin, then the ecophysiological behaviour, and finally the water balance.

4.1   Hydrological behaviour of the basin

The time series of streamflow Q and rainfall R are given at a semi-hourly time-step in Fig. 5a for 2009. Rainfall (Fig. 2) was quite evenly distributed (no marked dry spell), although the period from January to June clearly received less rain (later named the 'drier season', in opposition to the 'wetter season'). From the total R (3208 mm), the measured Q at the outlet was 2048 mm, yielding an annual streamflow coefficient of 0.64. The Q hydrograph (Fig. 5a) displays a continuous baseflow with episodes of groundwater recharge after rainfall events, followed by marked recessions controlled by the baseflow. Q peaks reached an annual maximum of 0.84 m^3 s^{-1}, i.e. 25 % of the nominal capacity of the flume, indicating that the size chosen for the flume was adequate. It can be observed that similar rainfall events resulted in much higher Q peaks during the wetter season. The lower Q peaks in response to rainfall events during the drier season could thus be interpreted as the consequence of higher infiltration rates when belowground was less saturated. Soil water content in the 0 - 1.6 m layer (Fig. 5d) remained above 37% all-year round and rose up to a maximum of 47% during the transition between the drier and the wetter season. In order to understand the large baseflow shaping the hydrograph of Q, four piezometers were installed in early June 2009 (Fig. 5e) and showed the existence of a permanent aquifer at levels varying between 0.7 and 3.2 m deep, according to their respective distance to water channels. Their behaviour was extremely variable, as expected, from responsive (piezos #1 and #3) to conservative behaviours (piezos #2 and #4). The continuous baseflow observed by the flume originated mainly from an important aquifer, covering a large (although undefined) area within the basin.

4.2 Ecophysiological behaviour of the basin

The ecosystem *LAI* index (Fig. 5*b*) changed seasonally quite severely from 2.8 (in March), as a result of coffee pruning during the drier season and leaf shedding by *E. poeppigiana*, coffee flowering and new leafing just after the beginning of the wetter season, to a maximum of 4.8 (in September), then coffee leaf shedding during the main coffee-berry harvest (in October).

The actual evapotranspiration (*ETR*) obtained by eddy-covariance (Fig. 5*c*) accounted for the sum of coffee and shade-tree transpiration, understory evaporation (mainly bare soil), and rainfall interception loss. The total *ETR* in 2009 accounted for 818 mm (25% of *R*), fluctuating daily according to atmospheric demand and seasonally according to *LAI* and canopy conductance. It remained always below 4.5 mm d^{-1} and, in average, around 60% of reference ET_0, i.e. clearly invalidating the use of ET_0 as a reliable indicator of *ETR* in coffee system hydrological models. The crop coefficient (the $ETR\ ET_0^{-1}$ ratio) was clearly lower during the drier season, as a consequence mainly of a lower *LAI*. We did not observe a period during which the relative extractable water (*REW*) of the soil drop below the critical value (REW_c) of 0.4, confirming that the coffee plants probably encountered no seasonal water stress.

4.3 Water balance partitioning and closure

Figure 6 shows the water balance partition and closure for 2009, as obtained by the water flows measured by independent experimental methods, rainfall (*R*), streamflow (*Q*), and evapotranspiration (*ETR*) (including the rainfall interception loss). It was observed on cumulative values that the sum of *Q*+*ETR* was 11% lower than annual *R*. However, *Q*+*ETR* matched or exceeded *R* once at the end of April, just after three episodes of lower rainfall, which confirmed the occurrence of an important storage in the basin, namely the soil and aquifer reservoirs, creating a seasonal hysteresis between *R* and *Q*. On an annual basis, measured *Q* represented 64% of *R* and measured *ETR* amounted 25%. The remaining 11% was attributed to deep percolation.

Figure 7*a* shows the result of the streamflow modelling for the year 2009, after calibrating the 10 parameters from Table 2. The model yielded a NS coefficient of 0.80 and $R^2 = 0.85$ for n = 17520 semi-hourly time-steps. Baseflow and peakflow events appeared to be satisfactorily represented for the whole time series. The modelled partitioning of streamflow into surface runoff, non-saturated runoff and baseflow (before routing) is presented in Fig. 7*b*. It indicated

1   a prominent contribution of baseflow, as already inferred from visual inspection of the Q time

2   series. Hillslope surface runoff was a minor part of Q. The water stored in the 4 lowest

3   reservoirs of the model is shown in Figs 7*c* to 7*f*. The water level at the surface reservoir was

4   rarely greater than zero, indicating rare events of surface storage (with runoff capacity)

5   beyond the time step (30 minutes). The non-saturated reservoirs showed rather stable

6   behaviours. Finally, the aquifer reservoir displayed the largest magnitude of variation,

7   fluctuating seasonally by a factor of almost 3.

8

5   Discussion

10   In the next sections we first discuss the validation, uncertainty and sensitivity analysis of the

11   model, then the main hydrological processes that we observed, and finally we examine the

12   hydrological services in our coffee AF basin.

5.1   Validation, uncertainty and sensitivity analysis for the Hydro-SVAT model

5.1.1 Model validation

15   Model validation was done by direct comparison of model output variables with three field

16   measurements: actual evapotranspiration *ETR*, soil water content θ and aquifer water level z.

17   For *ETR*, the determination coefficient between the daily sum of observed and modelled *ETR*

18   was R^2=0.79 (Fig. 8*a*). Concerning θ, the observed and modelled time series appeared to be

19   consistent, although not very precise in the driest season (Fig. 8*b*), reaching a rather low $R^2 =$

20   0.49. However, considering that this global θ was obtained as the arithmetic average of only

21   20 observations for the whole basin, the uncertainty of these measured values is high. The

22   large amount of rocks hindering the tubes might also affect the FDR readings. Finally, we

23   obtained a fair approximation for the behaviour of the aquifer (Fig. 8*c*), with R^2=0.90. The

24   use of the two piezometers that displayed the highest stability (i.e. probably representing a

25   larger volume of aquifer) out of the four installed piezometers was crucial at this step. We

26   considered to be recording two different processes, the typical gradual aquifer response

27   (piezos #2 and #4 in Fig. 1*c*) and the local quick-varying shallow-water accumulations (piezos

28   #1 and #3 in Fig. 1*c*), which might be associated with rapid changes in soil water contents at

29   smaller and less representative aquifer units. Though the representativeness of these few

30   piezometers of the behaviour of the main basin-aquifer could be questioned, the very high

1 similarity that we found between the modelled values and the average measurements from

2 piezometers #2 and #4 (located in two opposite ends of the basin), supported the idea of a

3 correct performance of both, the method for monitoring the aquifer and the corresponding

4 model routine based on a linear reservoir.

5 Concerning the precision of our model, the NS = 0.80 seems to be fair for a semi-hourly time-

6 step model, considering the detail with which the hydrological processes need to be described.

7 Some studies that have evaluated hydrological models using this coefficient for different time

8 scales have shown the decline in NS values as the modelling time step is shortened. For

9 instance, at calibration stages, Notter et al. (2007) achieved maximum NS values from 0.8 to

10 0.69 for decadal to daily time steps (basin area = 87 km^2), while Bormann (2006) obtained

11 0.8, 0.9, 0.85 and 0.73 for annual, monthly, weekly and daily time steps, respectively (basin

12 area = 63 km^2). García et al. (2008) reached NS coefficients of 0.93, 0.91 and 0.61 for

13 quarterly, monthly and daily evaluations in a 162 km^2 basin.

14 To study possible systematic errors in the Hydro-SVAT model, we examined the distribution

15 of residuals between measured and modelled streamflows (since this was the optimized

16 variable). A *t*-test indicated that the average of our residuals (equal to 3×10^{-4} m^3 s^{-1}) is

17 significantly different from zero for a confidence level CL=95% but not for a CL=99%

18 (*p*=0.02). Hence our model slightly underestimates the streamflow by 0.5% on average. At

19 our short time step it is common to find autocorrelations in residuals, so that we found

20 significant partial autocorrelations up to the eight time lag. The Kolmogorov-Smirnov test

21 revealed that the distribution of residuals is not normal (which is not desirable). Studying

22 residuals as functions of time, rainfall R, streamflow Q, soil water content θ and water table

23 level z (data not shown), we did not find any trends, but noticeable changes in their variability

24 make clear that the homoscedasticity condition was not properly fulfilled. However, it is

25 accepted that these ordinary least squares assumptions are often not satisfied (Xu and Singh,

26 1998).

5.1.2 Uncertainty analysis

28 If we accept that the model reproduces efficiently the actual streamflow at the outlet of the

29 experimental basin, the uncertainty in the modelled values needs to be known. A Monte-Carlo

30 (MC) uncertainty analysis was produced as detailed in Sect. 3.3 to yield the 95% and 99%

31 confidence limits (CL) around the modelled streamflow (the 99% CL are presented in Fig. 9,

1 along with measured streamflow). Though the modelled series was always close to the

2 observed one, only 20% of the measured values fell within the 95% CL produced by our

3 model, while 43% of them fell within the 99% CL. The ranges of the 95% confidence

4 intervals (CI) along each of the time steps varied from 5% to 57% of the MC mean value,

5 while for the 99% CI the ranges were from 11% up to 128% of the mean. From these analyses

6 it is possible to state that the model is efficient (high NS coefficient) and precise (small

7 confidence intervals, Fig. 9) modelling streamflow values, but is not highly accurate given the

8 low percentages of observed values falling within the 95% and 99% confidence intervals.

9 ### 5.1.3 Sensitivity analysis

10 The sensitivity analysis was carried out to determine the responsiveness of the model

11 predictions to variations in our main parameters. The first assessment consisted in testing the

12 statistical significance of the relationships between each of our 10 calibration parameters and

13 the NS coefficient, using four dimensionless sensitivity indexes: Pearson (PEAR), Spearman

14 (SPEA), standardized regression and standardized rank regression coefficients (SRC and

15 SRRC, respectively). Table 3 presents the results of these tests revealing that, with the

16 exception of the shallow-aquifer threshold E_X, none of the parameters seemed to significantly

17 influence the global model efficiency. However, these results may be misleading given the

18 enormously variable conditions under which the model works through time. Therefore, in a

19 second approach we selected the Spearman test (a simple rank transformation index that can

20 identify non linear relationships) to assess the influence of each of these 10 parameters on Q,

21 at each time step. Figure 10 presents the results, displaying the dimensionless Spearman index

22 in the vertical axis and the time in the horizontal axis. A positive Spearman index reveals a

23 proportional influence of the parameter on the model result, while negative values indicate

24 inverse proportionality. Figure 10a shows the time series for all the parameters, revealing an

25 alternation in their influence on Q over time and model state. The two black horizontal lines

26 represent the 95% confidence limits above (or below) which the correlation is significantly

27 different from zero. In Figs. 10b to 10k the significant values are plotted as black points in

28 contrast to non-significant in grey, for each parameter separately. Figure 10h suggests that the

29 parameter E_X is again one of the most influential, because it is permanently displaying high

30 positive or negative correlations, together with the discharge coefficient (DC) for the deep-

31 aquifer k_{E1}, which has a proportional influence on model outputs (Fig. 10j). These two

32 parameters reach the highest Spearman indexes during sustained periods (not only during

24

1   events) and are clearly relevant during long recessions, when the modelled water table level z

2   is around or below E_X. The DC for the surface reservoir k_B is noticeably influencing model

3   outputs but only during rainstorm events (Fig. 10c), while the DC for the deep percolation k_{E3}

4   (Fig. 10k) is significant during recessions. The vertical/lateral split coefficient β (Fig. 10b)

5   reaches high Spearman values when the non-saturated reservoirs are being recharged, in the

6   first stages of recessions when the humidity is above field capacity (directly proportional

7   effect), or else during the driest part of the recessions (inversely proportional effect). The DC

8   for the root reservoir k_C is significant when its humidity is higher than field capacity (Fig.

9   10f), while the DC for the shallow aquifer k_{E2} (Fig. 10i) has proportional influence when z if

10   above E_X or negative in the lowest part of the recessions. Finally, the infiltration rate at field

11   capacity (*fc*), the coefficient for maximum infiltration rate (α) and the DC for non-root

12   reservoir (k_D) seem to have no relevant effects on the Q modelling (Figs. 10d, 10e and 10g,

13   respectively).

5.2   Hydrological processes in the experimental basin

15   The main hydrological processes and components observed using this measuring/modelling

16   approach are presented in the following four sub-sections.

5.2.1 Interception, throughfall, stemflow and surface runoff

18   A review of water balance (WB) partitioning in comparable situations is proposed in Table 4

19   (interception loss, evapotranspiration, surface/non-saturated runoff, baseflow, change in soil

20   water content and deep percolation). In our basin, the adjusted interception loss (R_{In}) equalled

21   4% of input rainfall (R). This value is the same as found by Imbach et al. (1989) in a WB

22   experiment under similar coffee and *E. poeppigiana* land cover, but is lower than other

23   reports obtained by direct measurements at plot scale in Costa Rica: Jiménez (1986) found

24   16% under the same AF system; Harmand et al. (2007) found 15% for coffee and *Eucalyptus*

25   *deglupta* (but this R_{In} could be lower because stemflow was not separately measured); Siles

26   (2007) found 11-15% under coffee and *Inga densiflora*. Interception loss can be greatly

27   affected by the local *LAI* of both layers, the specific architecture of the coffee and trees and

28   the rainfall regime.

29   From the throughfall/stemflow component in our model (equal to 96% of R), 5% of R came

30   out of the basin as surface runoff Q_B. This value is not far from other reports at plot scale, like

31   those by Ávila et al. (2004): 1-9% (coffee and *E. deglupta*); Harmand et al. (2007): 2% and

1   Siles (2007): 3-6% (coffee and *I. densiflora*). At basin scale, Fujieda et al. (1997) measured

2   5% on a 0.56 km^2 basin under a three layer forest in Brazil, Lesack (1993) modelled 3% in a

3   rain-forest basin in Brazil (area: 0.23 km^2), Kinner et al. (2004) modelled 4% in a Panamanian

4   tropical-forest basin (0.10 km^2) and Charlier et al. (2008) modelled 10% in a banana-

5   plantation basin in Guadeloupe (0.18 km^2). A major source of surface runoff and discrepancy

6   between plot and basin scale studies could be the presence of roads. In our experimental basin

7   the total length of roads is 10 km and it represents 4.5% of the basin area. Then, assuming a

8   nil infiltration, runoff on roads and ditches could represent up to 67% of the total surface

9   runoff.

10   **5.2.2 Infiltration and drainage**

11   The non-intercepted and non-runoff fraction of incident rainfall was infiltrated ($i = 91\%$ of R).

12   This large i/R ratio and a Q_B/i ratio close to 5% give indication of very high infiltration and

13   drainage capacities, which are typical of andic-type volcanic soils (Poulenard et al. 2001,

14   Cattan et al., 2006) and are further enhanced for perennial crops in the absence of tillage and

15   in presence of substantial macroporosity (Dorel et al., 2000). This was pointed out by

16   preliminary measurements carried out in our experimental basin with a Cornell infiltrometer

17   (Ogden et al., 1997) that steady state infiltrability values were as high as 4.7×10^{-5} m s^{-1} (168

18   mm h^{-1}) (Kinoshita, pers. comm.). Recent experiments found hydraulic conductivity values as

19   high as 3.4×10^{-5} m s^{-1} (122 mm h^{-1}) and 2.1×10^{-5} m s^{-1} (75 mm h^{-1}) for andisols in Costa Rica

20   (Cannavo et al., in prep.) and Guadeloupe (Charlier et al., 2008), respectively. From our

21   infiltration capacity (that was modelled as a function of soil water content in the non-saturated

22   reservoirs), we calculated the infiltration/rainfall (i/R) and the runoff/infiltration (Q_B/i) ratios

23   at the storm-event scale, analyzing 78 events with cumulative rain higher than 10 mm. No

24   significant changes were found in any of these two ratios as a function of time (or season),

25   and only slight reductions were detected for increasing storm cumulative rainfall or soil water

26   content. This fact, added to the permanently high i/R ratios for each individual event (65-

27   98%), are explained by the constantly high infiltration capacity of andisols and the stable

28   behaviour of soil water content throughout the year. We therefore observed very efficient soil

29   and aquifer recharge mechanisms (Fig. 7*d* to 7*f*). According to Dorel et al. (2000) the soil

30   properties of non-tilled perennial crops in andisols are mainly determined by wetting-drying

31   cycles and by biological activity in the soil. Those are relatively stable factors in our

1 experimental basin, given the absence of a well-defined dry season on this side of the country

2 (Caribbean influence), and the permanently high organic matter content in these soils.

5.2.3 Evaporation and transpiration

4 Transpiration of coffee plants and trees T accounts for 21% of R (obtained from modelling).

5 Similar values for transpiration (23%) were reported by van Kanten and Vaast (2006) in

6 various coffee AF systems, while Siles (2007) measured higher values ranging from 28 to

7 34% (Table 4). In other experimental plots in Costa Rica, estimations of T ranged from 42 and

8 53% (Imbach et al., 1989 and Jiménez, 1986 respectively). T can be highly dependent on local

9 ET_0, on the effect of drought on stomatal closure, and on LAI. For a better site comparison, we

10 computed a simple "normalized transpiration" index $NT = T (ET_0 \ LAI)^{-1}$ in Table 4 and found

11 that our value (0.16) is very close to the respective ratio in the study of Siles (2007). As

12 mentioned earlier, we measured the actual evapotranspiration ($ETR=T+Eu+R_{In}$) in our

13 experimental basin by the eddy-covariance method and it represented 25% of R. This is the

14 smallest value reported in comparison to the other studies on coffee AF systems (Table 4).

15 The closest value (38%) was measured by Harmand et al. (2007), but it is about 1.5 times our

16 ETR, while a maximum of 69% was reported by Jiménez (1986). It must be stressed that our

17 study is the only one that brings independent validation of ETR through energy balance

18 closure, whereas many plot studies might carry errors due to the calibration of sapflow, the

19 model of E_u or the sampling of R_{In}. At the basin scale, many authors modelled ETR values

20 around 30% and 40% in tropical experimental basins (Lesack, 1993; Fujieda et al, 1997;

21 Genereux et al., 2005; Charlier et al., 2008).

5.2.4 Drainage and streamflow

23 Another component of interest at plot scale is drainage (vertical flow beyond root reservoir),

24 which we modelled as 61% of R and seems, on average, slightly higher than the values

25 reported in the literature (Table 4). The modelled deep percolation (or subsurface outflow

26 downstream the basin outlet) was 11%, much lower than the 42% reported by Charlier et al.

27 (2008), but similar to the 6% encountered by Kinner et al. (2004). As deep percolation is

28 calculated from water balance closure, its accuracy is enhanced when Q and ETR are precisely

29 measured.

30 The first or the second highest WB basin output is usually streamflow Q, which in our

31 experimental basin was recorded as 64% of R and modelled as 62%. It seems to be very close

1   to similar measurements in the tropics (Table 4). The baseflow from the aquifer accounted for

2   63% of total Q, while surface runoff was only 8% and non-saturated runoff 29%.

5.3   The coffee agroforestry basin and hydrological services

4   Modelling the hydrological behaviour of this experimental, coffee AF basin gave some

5   insights on the provision of HES by this system. This is particularly relevant in the Costa

6   Rican context where HES payments have already been implemented as national

7   environmental protection policies (Pagiola, 2008). Two main services related to water quality

8   can be recognized, both linked to the observed high infiltration i (91% of R) and low surface

9   runoff Q_B (5% of R).

10   At first, the low Q_B in the basin is closely associated to low surface displacement of fertilizers,

11   pesticides and sediments (Cattan et al., 2006, 2009; Leonard and Andrieux, 1998, Bruijnzeel,

12   2004). We found very constant Q_B/i ratios through the time, or under different rainfall

13   intensities, which may come from the expected stability in soil hydraulic properties (e.g. high

14   infiltration capacity) and the absence of either a marked dry season that controls soil

15   desiccation (Park and Cameron, 2008; Dorel et al., 2000) or mechanized agricultural practices

16   like tillage affecting soil compaction, surface roughness, continuity of pores, macroporosity,

17   soil cover and organic matter content (Le Bissonnais et al., 2005; Chahinian et al., 2006).

18   However, the high drainage capacity of these andisols might be a disadvantage in terms of

19   percolation and groundwater contamination by agrochemicals (Cattan et al., 2007; Saison et

20   al., 2008) given our model estimates for groundwater recharge of around 52% of R. In

21   addition, the modelled surface runoff for the experimental basin includes possible discharges

22   from unpaved roads and ditches, which needs to be controlled to avoid excessive water,

23   sediment and contaminant flux concentrations.

24   A second HES might be the streamflow regulation function provided by this AF basin through

25   aquifer recharge/discharge mechanisms. With a measured evapotranspiration close to 25% of

26   R (which is presumably much lower than the equivalent for forests), soil and aquifer water

27   depletion seems unlikely under the observed hydrogeological and climatic conditions,

28   favouring water availability during dry seasons (Robinson et al., 2003; Bruijnzeel, 2004). On

29   the other hand, during intense rainfalls and tropical storms the aquifer is efficiently recharged,

30   as we have observed in our piezometric measurements. The result is a homogeneous seasonal

31   distribution of streamflow, with a high rainfall recuperation fraction of 64% (Q/R).

6 Conclusions

This paper gives some insights on the assessment of HES by studying the hydrological processes in a particular micro-basin. The water balance partition is proposed as a baseline for analyses and negotiations leading to the payment of HES, for which measuring and modelling approaches are complementary. The understanding of water dynamics gave clear insights on the main services provided by the studied ecosystem, as well as some potential vulnerabilities.

The general behaviour of the coffee AF basin (1 km^2) on andisols can be summarized by the fact that 91% of R was infiltrated through the highly permeable andisol, 64% of R was measured as streamflow, 25% of R was measured as evapotranspiration, no major seasonal water stock variation in the soil and a high contribution of the aquifer to the streamflow as baseflow (Fig. 7b). These are characteristics of a system prone to generate important HES at basin scale, which is a result infrequently reported for coffee systems.

We proposed an original modelling approach coupling a hydrological and a SVAT model, calibrated using the streamflow at outlet of the basin but validated by independent and direct measurements of evapotranspiration, soil water content and water table level. These comprehensive measurements also allowed supporting the hypothesis of having an 11% of R as deep percolation.

We presented a standard uncertainty analysis and developed a simple method to built generic confidence intervals around our modelled streamflow values, as well as a sensitivity analysis to investigate the source of such uncertainty. The first parameterization of the model is considered adequate, though model simplification could be attempted centred on the two less sensitive parameters. Special attention needs to be given to direct measurement of a representative field capacity and the associated probability distribution function.

The conceptual nature of our Hydro-SVAT model allows a wide time/space domain of application, conditional only on knowledge of some general properties of the basin of interest and on the acquisition of basic hydrological data. Different environments can be configured in terms of climate, land cover, soils and hydrogeology, and further applications under different conditions are desired to test the generality of the model. Complementary studies like hillslope and channel surface runoff, basin water losses through roads, temporal variation in

29

soil and ecophysiological properties and ground water dynamics and composition are expected.

References

Anderson, E. P., Pringle, C. M. and Rojas, M.: Transforming tropical rivers: An environmental perspective on hydropower development in Costa Rica, Aquat. Conserv., 16, 679-693, 2006.

Ataroff, M., Monasterio, M.: Soil erosion under different management of coffee plantations in the Venezuelan Andes, Soil Technol., 11, 95-108, 1997.

Ávila, H., Harmand, J. M., Dambrine, E., Jiménez, F., Beer, J. and Oliver, R.: Dinámica del nitrógeno en el sistema agroforestal Coffea arabica con Eucalyptus deglupta en la Zona Sur de Costa Rica, Agroforestería en las Américas, 41-42, 83-91, 2004.

Baldocchi, D. and Meyers, T.: On using eco physiological, micrometeorological and biogeochemical theory to evaluate carbon dioxide, water vapor and trace gas fluxes over vegetation: a perspective, Agr. Forest Meteorol., 90, 1-25, 1998.

Bergström, S.: The HBV model, in: Computer Models of Watershed Hydrology, edited by: Singh, V. P., Water Resources Publications, Colorado, USA, 1995.

Bormann, H.: Impact of spatial data resolution on simulated catchment water balances and model performance of the multi-scale TOPLATS model, Hydrol. Earth Syst. Sc., 10, 165-179, 2006.

1   Bruijnzeel, L. A.: Hydrological functions of tropical forests: not seeing the soil for the trees?,
2   Agr. Ecosyst. Environ., 104, 185-228, 2004.

3   Cannavo, P., Sansoulet, J., Siles, P., Harmand, J. M., Dreyer, E. and Vaast, P.: Estimation of
4   water use and modelling water balance in a coffee (Coffea Arabica L.) plantation shaded with
5   Inga densiflora in Costa Rica, in prep.

6   Cattan, P., Cabidoche, Y. M., Lacas, J. G and Voltz, M.: Effects of tillage and mulching on
7   runoff under banana (Musa spp.) on a tropical Andosol, Soil Till. Res., 86, 38-51, 2006.

8   Cattan, P., Voltz, M., Cabidoche, Y. M., Lacas, J. G. and Sansoulet, J.: Spatial and temporal
9   variations in percolation fluxes in a tropical Andosol influenced by banana cropping patterns,
10   J. Hydrol., 335, 157-169, 2007.

11   Cattan, P., Ruy, S. M., Cabidoche, Y. M., Findeling, A., Desbois, P. and Charlier, J. B.: Effect
12   on runoff of rainfall redistribution by the impluvium-shaped canopy of banana cultivated on
13   an Andosol with a high infiltration rate, J. Hydrol., 368, 251-261, 2009.

14   Ceballos, A. and Schnabel, S.: Hydrological behaviour of a small catchment in the dehesa
15   land-use system (Extremadura, SW Spain), J. Hydrol., 210, 146-160, 1998.

16   Chahinian, N., Moussa, R., Andrieux, P. and Voltz, M.: Comparison of infiltration models to
17   simulate flood events at the field scale, J. Hydrol., 306, 191-214, 2005.

18   Chahinian, N., Moussa, R., Andrieux, P. and Voltz, M.: Accounting for temporal variation in
19   soil hydrological properties when simulating surface runoff on tilled plots, J. Hydrol., 326,
20   135-152, 2006.

21   Charlier, J. B., Cattan, P., Moussa, R. and Voltz., M.: Hydrological behaviour and modelling
22   of a volcanic tropical cultivated catchment, Hydrol. Process., 22, 4355-4370, 2008.

23   Cormary, Y. and Guilbot, A.: Relations pluie-débit sur le bassin de la Sioule, Rapport
24   D.G.R.S.T. N° 30, Université des Sciences et Techniques, Montpellier, France, 1969.

25   Crawford, N. H. and Linsley, R. K.: Digital simulation in hydrology: Stanford watershed
26   model IV, Technical Report 39, Department of Civil Engineering, Stanford University,
27   Stanford, California, 1966.

28   Dauzat, J., Rapidel, B. and Berger, A.: Simulation of leaf transpiration and sap flow in virtual
29   plants: model description and application to a coffee plantation in Costa Rica, Agr. Forest
30   Meteorol., 109, 143-160, 2001.

Dawes, W. R., Zhang, L., Hatton, T. J., Reece, P. H., Beale, G.T.H. and Packer, I.: Evaluation of a distributed parameter ecohydrological model (TOPOG_IRM) on a small cropping rotation catchment, J. Hydrol., 191, 64-86, 1997.

Diskin, M. and Nazimov, N.: Linear reservoir with feedback regulated inlet as a model for the infiltration process, J. Hydrol., 172, 313-330, 1995.

Donigan, A., Bicknell, B. and Imhoff, J. C.: Hydrological simulation program – Fortran (HSPF), in: Computer Models of Watershed Hydrology, edited by: Singh, V. P., Water Resource Publications, Colorado, USA, 1995.

Dorel, M., Roger-Estrade, J., Manichon, H. and Delvaux, B.: Porosity and soil water properties of Caribbean volcanic ash soils, Soil Use Manage., 16, 133-140, 2000.

Duan, Q., Sorooshian, S. and Gupta, V.: Effective and efficient global optimisation for conceptual rainfall-runoff models, Water Resour. Res., 28, 1015-1031, 1992.

Falge, E., Baldocchi, D., Olson, R., Anthoni, P., Aubinet, M., Bernhofer, C., Burba, G., Ceulemans, R., Clement, R., Dolman, H., Granier, A., Gross, P., Grünwald, T., Hollinger, D., Jensen, N.-O., Katul, G., Keronen, P., Kowalski, A., Ta Lai, C., Law, B. E., Meyers, T., Moncrieff, J., Moors, E., William Munger, J., Pilegaard, K., Rannik, Ü., Rebmann, C., Suyker, A., Tenhunen, J., Tu, K., Verma, S., Vesala, T., Wilson, K., and Wofsy, S.: Gap filling strategies for long term energy flux data sets, Agr. Forest Meteorol., 107, 71-77, 2001.

FAO: Crop evapotranspiration, Guidelines for computing crop water requirements, FAO drainage and irrigation papers, 56, 1998.

Fleming, G.: Computer simulation techniques in hydrology, Environmental Science Series, Elsevier, New York, USA, 1975.

Fujieda, M., Kudoh, T., de Cicco, V. and de Calvarcho, J. L.: Hydrological processes at two subtropical forest catchments: the Serra do Mar, São Paulo, Brazil, J. Hydrol., 196, 26-46, 1997.

García, A., Sainz, A., Revilla, J. A., Álvarez, C., Juanes, J. A. and Puente, A.: Surface water resources assessment in scarcely gauged basins in the north of Spain, J. Hydrol., 356, 312-326, 2008.

1   Genereux, D. P., Jordan, M. T. and Carbonell, D.: A paired-watershed budget study to
2   quantify interbasin groundwater flow in a lowland rain forest, Costa Rica, Water Resour.
3   Res., 41, W04011, 2005.

4   Granier, A., Breda, N., Biron, P. and Villette, S.: A lumped water balance model to evaluate
5   duration and intensity of drought constraints in forest stands. Ecol. Model., 116, 269-283,
6   1999.

7   Gutiérrez, M. V., Meinzer, F. C. and Grantz, D. A.: Regulation of transpiration in coffee
8   hedgerows: covariation of environmental variables and apparent responses of stomata to wind
9   and humidity, Plant Cell Environ., 17, 1305-1313, 1994.

10   Hamby, D. M.: A review of techniques for parameter sensitivity analysis of environmental
11   models, Environ. Monit. Assess., 32, 135-154, 1994.

12   Hamby, D. M.: A comparison of sensitivity analysis techniques, Health Phys., 68, 195-204,
13   1995.

14   Helton, J. C.: Uncertainty and sensitivity analysis in performance assessment for the Waste
15   Isolation Pilot Plant, Comput. Phys. Commun., 117, 156-180, 1999.

16   Harmand, J. M., Ávila, H., Dambrine, E., Skiba, U., de Miguel, S., Renderos, R. V., Oliver,
17   R., Jiménez, F. and Beer, J.: Nitrogen dynamics and soil nitrate retention in a Coffea arabica -
18   Eucalyptus deglupta agroforestry system in southern Costa Rica, Biogeochemistry, 85, 125-
19   139, 2007.

20   Havnø, K., Madsen, M. N. and Dørge, J.: MIKE 11 – a generalized river modelling package,
21   in: Computer Models of Watershed Hydrology, edited by: Singh, V. P., Water Resources
22   Publications, Colorado, 1995.

23   Hodnett, M. G., and Tomasella, J.: Marked differences between van Genuchten soil water-
24   retention parameters for temperate and tropical soils: a new water- retention pedo-transfer
25   functions developed for tropical soils, Geoderma, 108, 155-180, 2002.

26   ICE (Instituto Costarricense de Electricidad): Plan de Expansión de la Generación Eléctrica,
27   Período 2010-2021, San José, Costa Rica, 2009.

28   Imbach, A. C., Fassbender, H. W., Beer, J., Borel, R. and Bonnemann, A.: Sistemas
29   agroforestales de café (Coffea arabica) con laurel (Cordia alliodora) y café con poró

(Erythrina poeppigiana) en Turrialba, Costa Rica. VI. Balances hídricos e ingreso con lluvias y lixiviación de elementos nutritivos, Turrialba (IICA), 39, 400-414, 1989.

Jiménez, F.: Balance hídrico con énfasis en percolación de dos sistemas agroforestales: café-poró y café-laurel, en Turrialba, Costa Rica, MSc Thesis, Universidad de Costa Rica, Centro Agronómico Tropical de Investigación y Enseñanza, Turrialba, Costa Rica, 1986.

Kinner, D. A. Stallard, R. F.: Identifying storm flow pathways in a rainforest catchment using hydrological and geochemical modelling, Hydrol. Process., 18, 2851-2875, 2004.

Le Bissonnais, Y., Cerdan, O., Lecomte, V., Benkhadra, H., Souchère, V. and Martin, P.: Variability of soil surface characteristics influencing runoff and interrill erosion, Catena, 62, 111-124, 2005.

Leonard, J. and Andrieux, P.: Infiltration characteristics of soils in Mediterranean vineyards in Southern France, Catena, 32, 209-223, 1998.

Lesack, L. F. W.: Water Balance and hydrologic characteristics of a rain forest catchment in the Central Amazon basin, Water Resour. Res., 29, 759-773, 1993.

Maeda, K., Tanaka, T., Park, H. and Hattori, S.: Spatial distribution of soil structure in a suburban forest catchment and its effect on spatio-temporal soil moisture and runoff fluctuations, J. Hydrol., 321, 232-256, 2006.

Marsden, C., le Maire, G., Stape, J. L., Seen, D. L., Roupsard, O., Cabral, O., Epron, D., Lima, A. M. N. and Nouvellon, Y.: Relating MODIS vegetation index time-series with structure, light absorption and stem production of fast-growing Eucalyptus plantations, Forest Ecol. Manag., 259, 1741-1753, 2010.

Millennium Ecosystem Assessment (MEA): Ecosystems and human well-being: synthesis, Island Press, Washington DC, USA. 2005.

MINAE-RECOPE: Mapa geológico de Costa Rica, Scale: 1:200000, San José, Costa Rica, 1991.

Mora-Chinchilla, R.: Geomorfología de la cuenca del Río Turrialba (unpublished), Universidad de Costa Rica, San José, Costa Rica, 2000.

Moussa, R., Chahinian, N. and Bocquillon, C.: Distributed hydrological modelling of a Mediterranean mountainous catchment - model construction and multi-site validation, J. Hydrol., 337, 35-51, 2007a.

1   Moussa, R., Chahinian, N. and Bocquillon, C.: Erratum to "Distributed hydrological

2   modelling of a Mediterranean mountainous catchment - model construction and multi-site

3   validation" [J. Hydrol., 337, 35-51, 2007], J. Hydrol., 345, 254, 2007b.

4   Moussa, R. and Chahinian, N.: Comparison of different multi-objective calibration criteria

5   using a conceptual rainfall-runoff model of flood events, Hydrol. Earth Syst. Sc., 13, 519-535,

6   2009.

7   Nash, I. E. and Sutcliffe, J. V.: River flow forecasting through conceptual models. Part I: a

8   discussion of principles, J. Hydrol., 10, 282-290, 1970.

9   Nilson, T.: A theoretical analysis of the frequency of gaps in plant stands, Agr. Meteorol., 8,

10   25-38, 1971.

11   Notter, B., MacMillan, L., Viviroli, D., Weingartner, R. and Liniger, H.: Impacts of

12   environmental change on water resources in the Mt. Kenya region, J. Hydrol., 343, 266-278,

13   2007.

14   Ogden, C. B., van Es, H. M. and Schindelbeck, R. R.: Miniature rain simulator for field

15   measurement of soil infiltration, Soil Sci. Soc. Am. J., 61, 1041-1043, 1997.

16   Pagiola, S.: Payments for environmental services in Costa Rica, Ecol. Econ., 65, 712-724,

17   2008.

18   Park, A. and Cameron, J. L.: The influence of canopy traits on throughfall and stemflow in

19   five tropical trees growing in a Panamanian plantation, Forest Ecol. Manag., 255, 1915-1925,

20   2008.

21   Peel, M. C., Finlayson, B. L. and McMahon, T. A.: Updated world map of the Köppen-Geiger

22   climate classification, Hydrol. Earth Syst. Sc., 11, 1633-1644, 2007.

23   Poulenard, J., Podwojewski, P., Janeau, J. L. and Collinet, J.: Runoff and soil erosion under

24   rainfall simulation of Andisols from the Ecuadorian Páramo: effect of tillage and burning,

25   Catena, 45, 185-207, 2001.

26   Roberts, G. and Harding, R. J.: The use of simple process-based models in the estimate of

27   water balances for mixed land use catchments in East Africa, J. Hydrol., 180, 251-266, 1996.

28   Robinson, M., Cognard-Plancq, A.L., Cosandey, C., David, J., Durand, P., Führer, H. W.,

29   Hall, R., Hendriques, M. O., Marc, V., McCarthy, R., McDonnell, M., Martin, C., Nisbet, T.,

O'Dea, P., Rodgers, M. and Zollner, A.: Studies of the impact of forests on peak flows and baseflows: a European perspective, Forest Ecol. Manag., 186, 85-97, 2003.

Roupsard, O., Bonnefond, J. M., Irvine, M., Berbigier, P., Nouvellon, Y., Dauzat, J., Taga, S., Hamel, O., Jourdan, C., Saint-Andre, L., Mialet-Serra, I., Labouisse, J. P., Epron, D., Joffre, R., Braconnier, S., Rouziere, A., Navarro, M. and Bouillet, J.P.: Partitioning energy and evapo-transpiration above and below a tropical palm canopy, Agr. Forest Meteorol., 139, 252-268, 2006.

Roupsard, O., Dauzat, J., Nouvellon, Y., Deveau, A., Feintrenie, L., Saint-Andre, L., Mialet-Serra, I., Braconnier, S., Bonnefond, J. M., Berbigier, P., Epron, D., Jourdan, C., Navarro, M. and Bouillet, J.P.: Cross-validating Sun-shade and 3D models of light absorption by a tree-crop canopy, Agr. Forest Meteorol., 148, 549-564, 2008.

Rouse, J. W., Haas, R. H., Schell, J. A. and Deering, D. W.: Monitoring vegetation systems in the Great Plains with ERTS, in: Proc. Third Earth Resources Tech. Satellite-1 Symp. Vol. 1: Technical Presentations, Sec. A, NASA SP-351, edited by: Freden, S. C., Mercanti, E. P. and Becker M. A., NASA Science and Technology Information Office, Washington, D.C., 309-317, 1974.

Ruiz, L., Varma, M. R. R., Kumar, M. S. M., Sekhar, M., Maréchal, J. C., Descloitres, M., Riotte, J., Kumar, S., Kumar, C. and Braun, J. J.: Water balance modelling in a tropical watershed under deciduous forest (Mule Hole, India): Regolith matric storage buffers the groundwater recharge process, J. Hydrol., 380, 460-472, 2010.

Saison, C., Cattan, P., Louchart, X. and Voltz, M.: Effect of spatial heterogeneities of water fluxes and application pattern on cadusafos fate on banana-cultivated andosols, J. Agr. Food Chem., 56, 11947–11955, 2008.

SEPSA (Secretaría Ejecutiva de Planificación Sectorial Agropecuaria): Boletín Estadístico Agropecuario, 19, ISSN 1659-1232, 2009.

Siles, P.: Hydrological processes (water use and balance) in a coffee (Coffea arabica L.) monoculture and a coffee plantation shaded by Inga densiflora in Costa Rica, PhD Thesis Dissertation, Université Henri Poincaré, Nancy, France, 2007.

Siles, P., Harmand, J. M. and Vaast, P.: Effects of Inga densiflora on the microclimate of coffee (Coffea arabica L.) and overall biomass under optimal growing conditions in Costa Rica. Agroforest. Syst., 78, 269-286, 2010.

1   Siles, P., Vaast, P., Dreyer, E. and Harmand, J. M.: Stemflow and rainfall interception in
2   coffee (Coffea arabica L.) in monoculture or shaded by Inga densiflora, J. Hydrol., in review.

3   Singh, V.P.: Computer Models of Watershed Hydrology, Water Resources Publications,
4   Colorado, 1995.

5   Sorooshian, S. and Gupta, V. K.: Model calibration, Chapter 2, in: Computer Models of
6   Watershed Hydrology, edited by: Singh, V. P., Water Resources Publications, Colorado,
7   USA, 1995.

8   Vaast, P., Beer, J., Harvey, C. and Harmand, J. M.: Environmental services of coffee
9   agroforestry systems in Central America: a promising potential to improve the livelihoods of
10 coffee farmers' communities, in: Intregrated Management of Environmental Services in
11 Human-Dominated Tropical Landscapes, edited by: CATIE, IV Henri A. Wallace Inter-
12 American Scientific Conference Series, Turrialba, Costa Rica, 35-39, 2005.

13 van Kanten, R. and Vaast, P.: Transpiration of arabica coffee and associated shade tree
14 species in sub-optimal, low-altitude conditions of Costa Rica, Agroforest. Syst., 67, 187-202,
15 2006.

16 Vega, F. E. and Rosenquist, E.: The coffee berry borer and coffee research at the United
17 States Department of Agriculture, in: Proc. World Coffee Conference, London, UK, 2001.

18 Wahl, T. L., Clemmens, A. J., Replogle, J. A. and Bos, M. G.: WinFlume - Windows-based
19 software for the design of long-throated measuring flumes, Fourth Decennial National
20 Irrigation Symposium, American Society of Agricultural Engineers, Phoenix, Arizona, 2000.

21 Wilson, K. B., Hanson, P. J., Mulholland, P. J., Baldocchi, D. D. and Wullschleger, S. D.: A
22 comparison of methods for determining forest evapotranspiration and its components: sap-
23 flow, soil water budget, eddy covariance and catchment water balance, Agr. Forest Meteorol.,
24 106, 153-168, 2001.

25 Xu, C.Y. and Singh, V. P.: A Review on Monthly Water Balance Models for Water
26 Resources Investigations, Water Resour. Manag., 12, 31-50, 1998.

1   Table 1. Measured hydrologic variables, record and gaps periods.

Variable	Frequency of measurement	Measurement period (2009)	Data gaps	Gap filling method
Rainfall R	10 minutes	01/01 - 31/12	No	-
Streamflow Q	10 minutes	01/01 - 18/07 23/07 - 31/12	18/07 - 23/07	Using the current model. Peak estimati on by peakflow/peak rainfall analysis
Measured evapotranspiration ETR	20 Hertz	04/03 - 17/07 30/08 - 31/12	01/01 - 04/03 17/07 - 30/08	Penman-Monteith model adjusting the canopy conductance
Soil water content θ	7 to 15 days	02/04 - 07/12	01/01 - 02/04	-
Water table level z	30 minutes	02/06 - 31/12	01/01 - 02/06	-

2   Table 2. Parameter description, range for optimization, optimized value and range for sensitivity analysis.

Parameter	Description	Units	Range for optimization	Reference	Optimum value
β	Vertical/lateral split coefficient to divide outputs from non-saturated reservoirs into non-saturated runoff and vertical flows	fraction	[0 - 0.84]	Moussa and Chahinian (2009)	0.106
k_B	discharge rate for surface reservoir	s^{-1}	$[0 - 1] \times 10^{-4}$	Empirical parameter	2.43×10^{-5}
fc	infiltration rate at field capacity	$m\ s^{-1}$	$[0 - 1] \times 10^{-5}$	Minimum steady state infiltrab. in the experim. basin (Kinoshita, pers. comm.)	2.48×10^{-7}
α	coefficient to calculate the maximum infiltration capacity from field capacity	dimensionless	[1 - 70]	Moussa and Chahinian (2009)	33.0
k_C	discharge coefficient, total outputs from non-saturated root reservoir	s^{-1}	$[0 - 1] \times 10^{-5}$	Empirical parameter	4.59×10^{-6}
k_D	discharge coefficient for total outputs from non-saturated non-root reservoir	s^{-1}	$[0 - 1] \times 10^{-5}$	Empirical parameter	6.55×10^{-5}
E_X	threshold level in the aquifer reservoir, above which a shallow-aquifer outlet is found	m	[0 - 1]	Empirical parameter	0.323
k_{E2}	discharge coefficient for baseflow from shallow aquifer reservoir	s^{-1}	$[0 - 2.4] \times 10^{-6}$	Charlier et al. (2008)	7.14×10^{-7}
k_{E1}	discharge coefficient for baseflow from deep aquifer reservoir	s^{-1}	$[0 - 2.1] \times 10^{-6}$	Charlier et al. (2008)	1.02×10^{-7}
k_{E3}	discharge coefficient for deep percolation from the aquifer reservoir	s^{-1}	$[0 - 1] \times 10^{-7}$	Empirical parameter	4.93×10^{-8}

3 Table 3. Sensitivity indexes for each of the 10 calibration parameters vs. the NS coefficient.
4 PEAR: Pearson product moment correlation coefficient, SPEA: Spearman coefficient, SRC:
5 Standardized regression coefficient and SRRC: Standardized rank regression coefficients.
6 Index values in bold are statistically significant at 95% confidence level.

Parameter	Sensitivity index			
	PEAR	SPEA	SRC	SRRC
β	-0.14	-0.13	-0.05	-0.03
k_B	**-0.16**	-0.10	-0.14	-0.07
fc	-0.01	0.04	-0.05	0.03
α	0.08	**0.22**	0.06	**0.22**
k_C	0.15	0.10	0.06	0.01
k_D	**0.16**	**0.19**	0.00	0.03
E_X	**-0.26**	**-0.22**	**-0.17**	**-0.12**
k_{E2}	-0.03	-0.08	0.02	-0.03
k_{E1}	0.15	0.15	0.13	**0.11**
k_{E3}	-0.13	-0.09	-0.10	-0.03

Table 4. Comparison of annual water balance components (as % of rainfall) for different studies at plot and basin scales, in tropical regions.

Source	Location	Climate	Basin area (km^2)	Land cover	LAI (m^2 m^{-2})	Rainfall R (mm)	R_{In}[a]	T[a]	Total ETR[a]	ET_0[a]	NT[d]	Q_B[a]	Q_{CD}[a]	Q_E[a]	Total Q[a]	ΔS[a]	D[a]	DP, SO[a]
Jiménez (1986)	Costa Rica	Humid tropical	plot scale	Coffee and *E. poeppigiana*	-	**2642**[b]	**16**	53	69	-	-	-	-	-	-	9	22	-
Imbach et al. (1989)	Costa Rica	Humid tropical	plot scale	Coffee and *E. poeppigiana*	-	**1919**	**4**	42	46	60	-	-	-	-	-	-	54	-
Harmand et al. (2007)	Costa Rica	Humid tropical	plot scale	Coffee and *E. deglupta*	3.5	**2622**[b]	**15**	**23**	**38**	-	-	2	-	-	-	6	54	-
Siles (2007), Cannavo et al. (in prep.)	Costa Rica	Humid tropical	plot scale	Coffee and *I. densiflora*	5.0-6.0	**2684-3245**	**11-15**	**28-34**	**41-46**	39-44	0.14	3-6	-	-	-	**-1-1**	44-55	-
Lesack (1993)	Brazil	Humid tropical	0.23	Rain forest	-	**2870**	-	-	39	-	-	3	-	-	**57**	**2**	-	1
Fujieda et al. (1997)	Brazil	Humid subtrop.	0.56	Three layer forest	-	**2319**	15	15	30	32	-	5	6	59	**70**	-	-	-
Kinner et al. (2004)	Panama	Humid tropical	0.10	Tropical forest	-	**2400**	-	-	53	56	-	4	17	20	**41**	6[c]	-	6[c]
Genereux et al. (2005)	Costa Rica	Humid tropical	0.26	Tropical rain forest	-	**4974**	-	-	32-46	-	-	-	-	-	**54-68**	-	-	-
Charlier et al. (2008)	Guadeloupe	Maritime hum. trop.	0.18	Banana	-	**4229**	-	-	31	31	-	10	-	17	**27**	0	59	42
This study	Costa Rica	Humid tropical	0.90	Coffee and *E. poeppigiana*	3.8	**3208**	4	21	**25**	32	0.16	5	18	39	62-**64**	0	61	11

* Numbers in bold are measured quantities.

[a] Given as % of R: R_{In}: interception loss, T: transpiration, *ETR*: evapotranspiration, ET_0: reference evapotranspiration, Q_B: surface runoff, Q_{CD}: non-saturated runoff (subsurface flow), Q_E: baseflow, Q: streamflow, D: drainage, ΔS: change in soil water content, *DP*: deep percolation, *SO*: subsurface outflow.

[b] Annual estimation for experiments conducted in short term periods (less than a year).

[c] The authors do not know whether this fraction is being stored in soil, or it became subsurface outflow downstream the gauging site.

[d] NT = normalized transpiration equal to $T (ET_0 LAI)^{-1}$
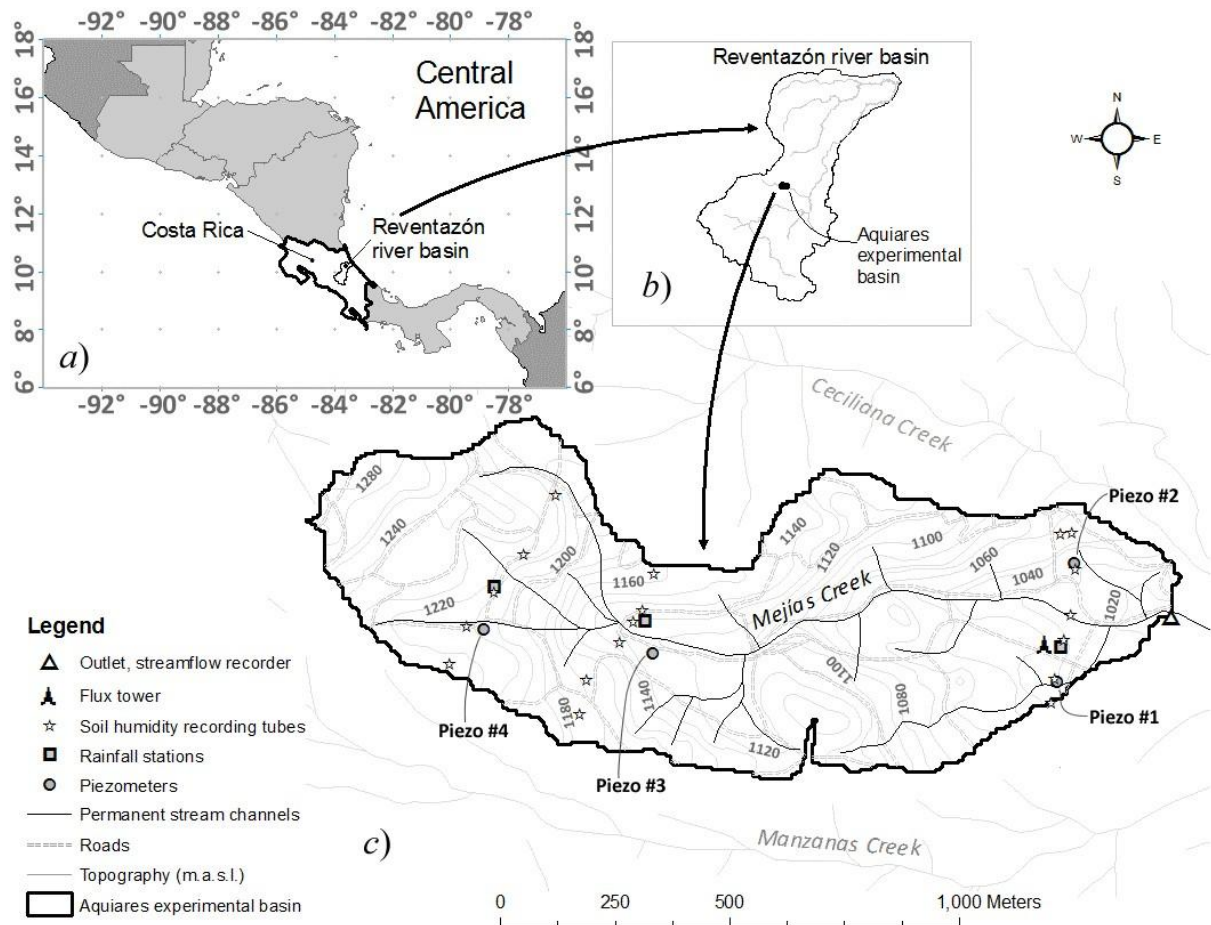
15

16

17 Figure 1. *a*) Location of Reventazón river basin in Costa Rica, Central America. *b*) Position of

18 experimental basin inside of Reventazón basin. *c*) The "Coffee-Flux" experimental basin in

19 Aquiares farm and its experimental setup to measure the water balance components.
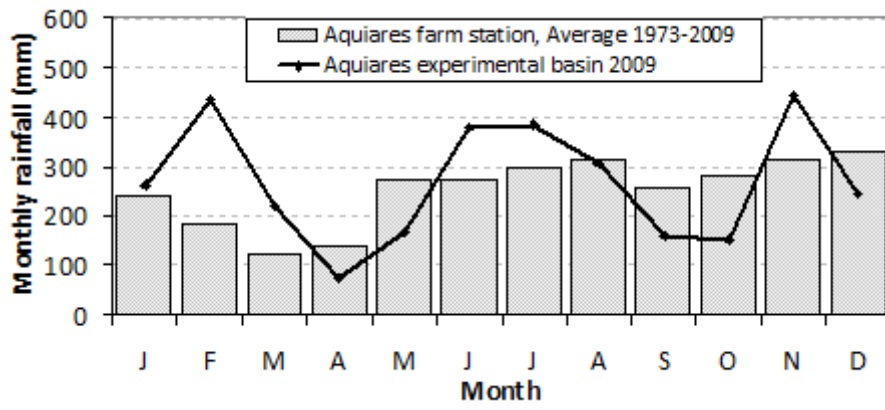
20

21

22   Figure 2. Mean monthly rainfall at Aquiares farm station (period 1973-2009) compared to the

23   rainfall in the experimental basin in 2009.
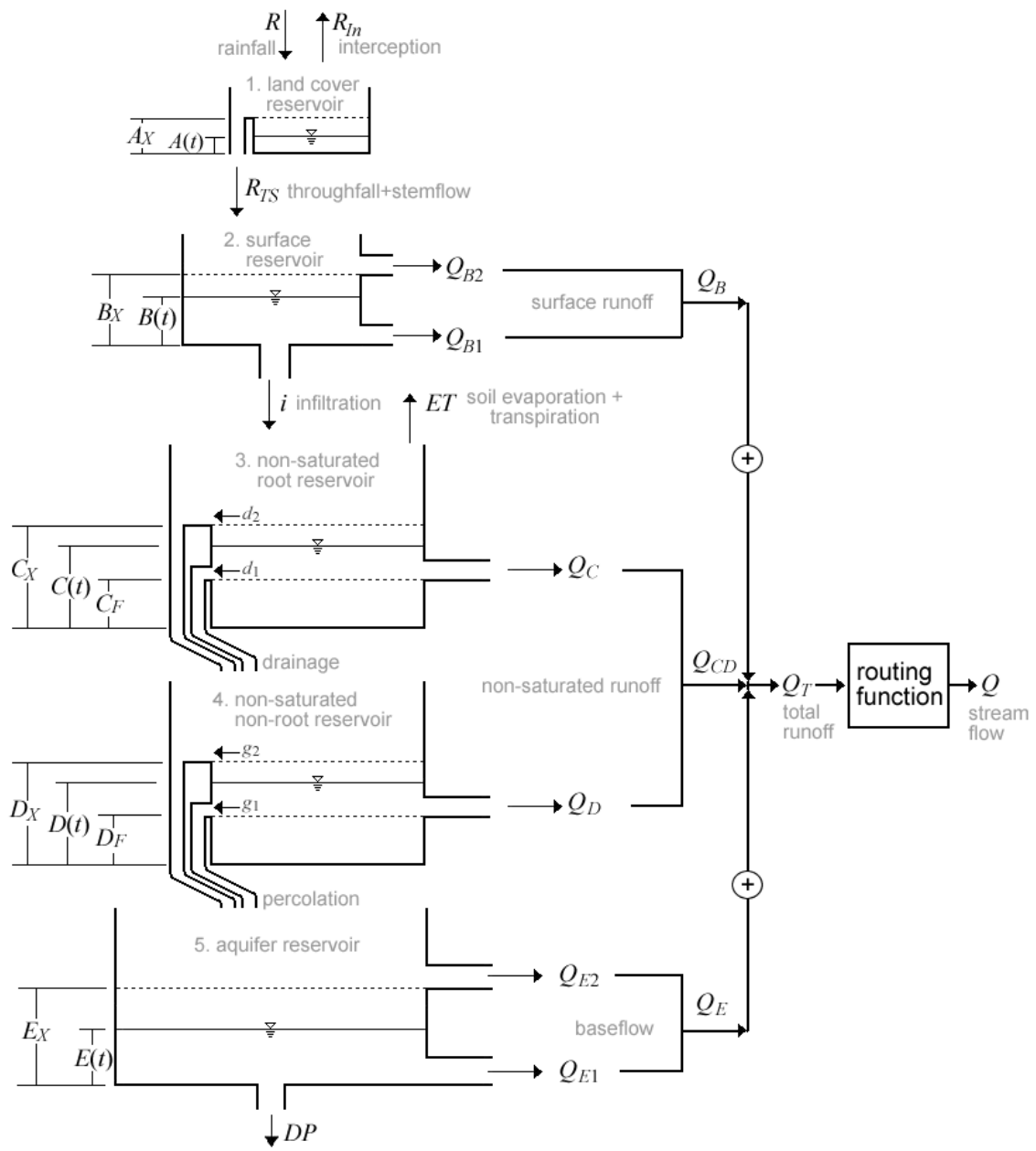
24

25

26   Figure 3. The lumped conceptual hydrological model proposed for the experimental basin.

27

28

29
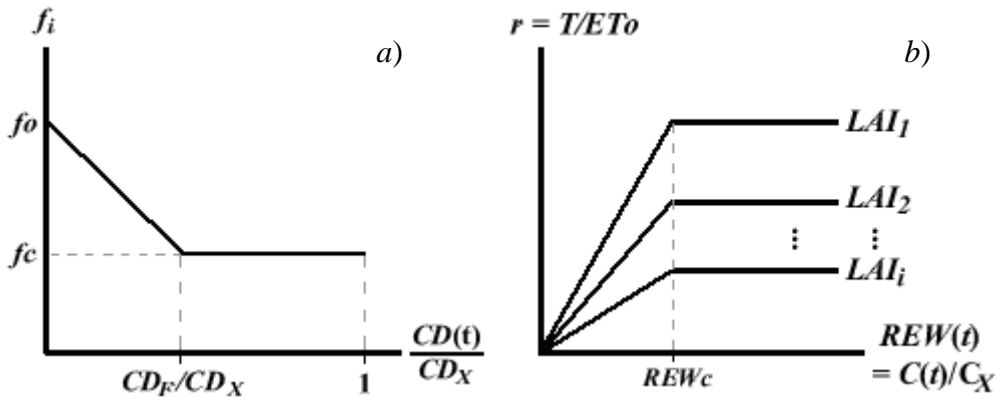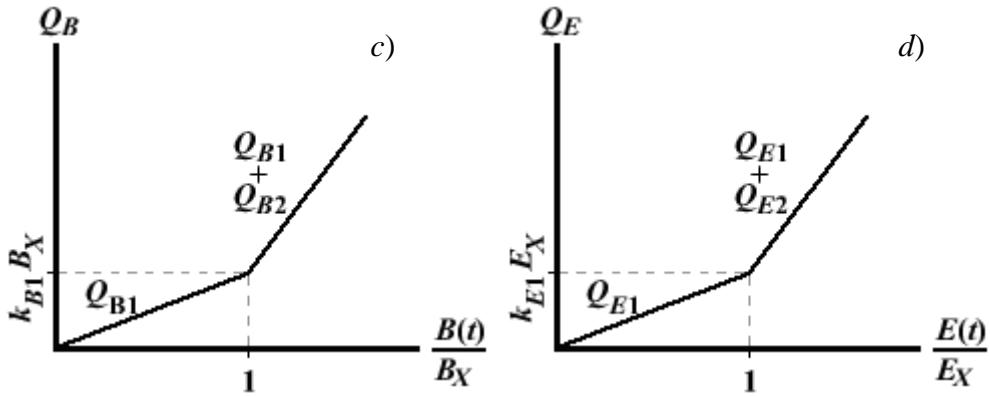
Figure 4. *a*) Infiltration from surface reservoir as a function of soil water content in non-saturated reservoirs, *b*) The ratio $r = T \, ET_0^{-1}$ as a function of relative extractable water *REW* and for different values of *LAI* (here, $LAI_1 > LAI_2 > \ldots > LAI_i$), *c*) Surface runoff from the surface reservoir as a function of its water content, *d*) Baseflow from the aquifer reservoir as a function of its water content.

35

36

37

38
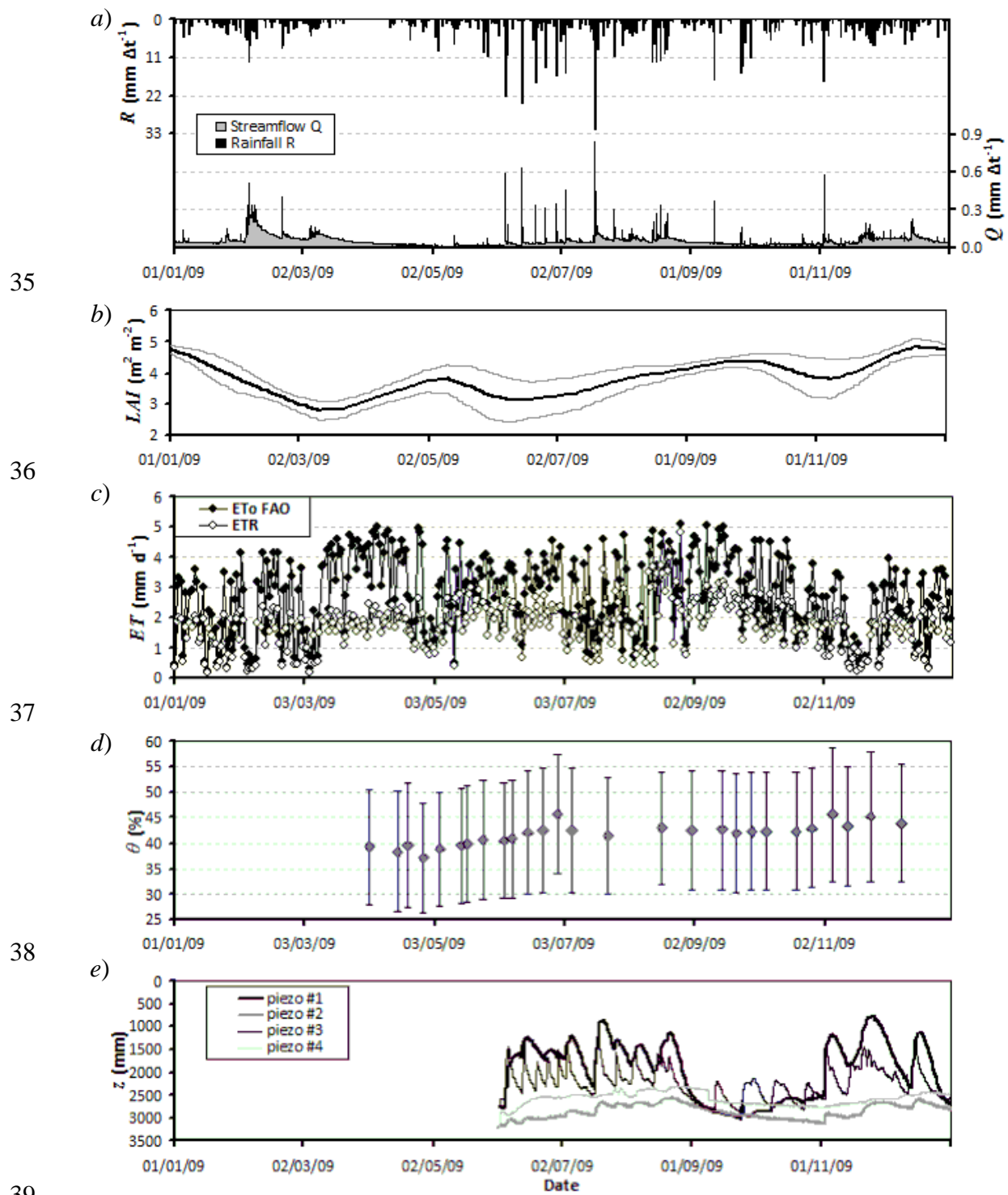
39

40

41   Figure 5. Measurements in the experimental basin for 2009: *a*) rainfall *R* and streamflow *Q*,

42   Δ*t*=30 min, *b*) leaf area index (*LAI*) within 1 std. dev. confidence bands (grey), *c*) reference-

43   potential (*ET₀*) and measured (*ETR*) daily evapotranspiration, *d*) soil water content *θ* with one

44   standard deviation bars and *e*) water table level *z* in the four piezometers throughout the basin.
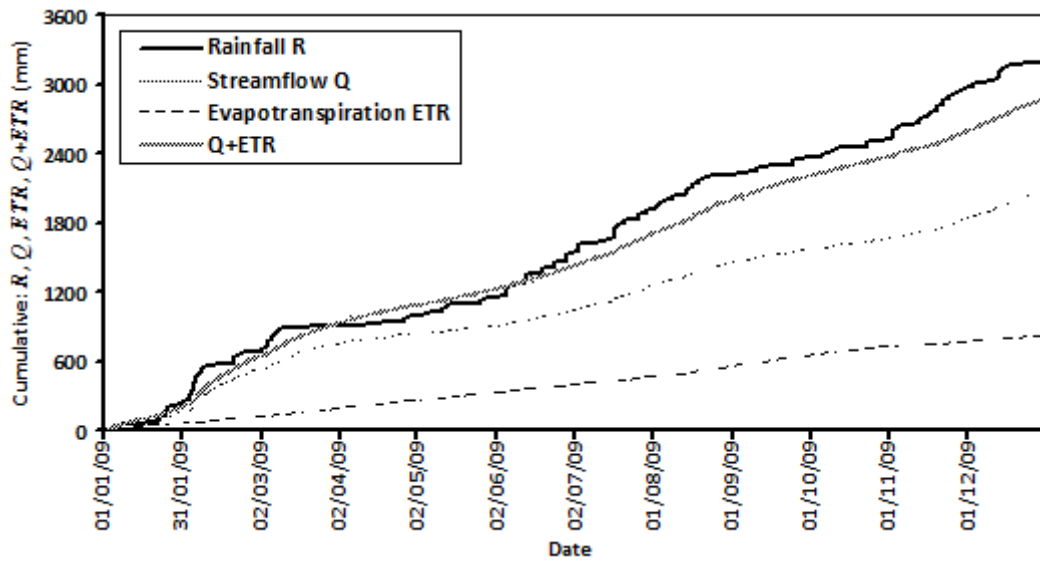
Figure 6. Water balance in the experimental basin for 2009. Only measured values are presented here.

49

50

51

52
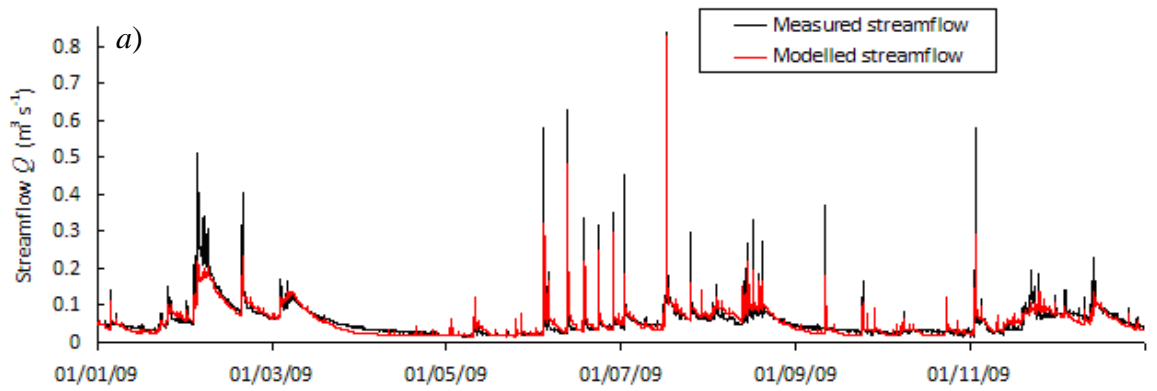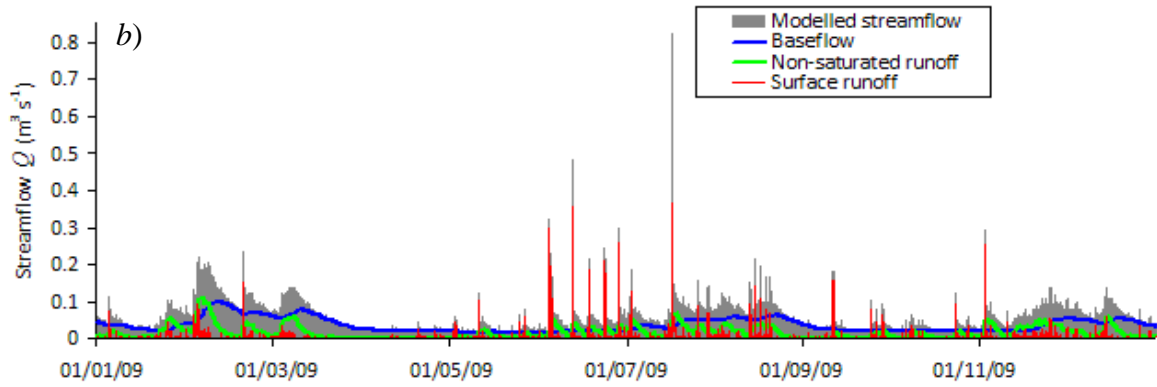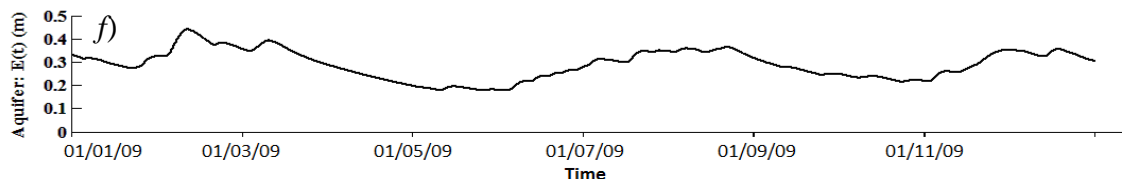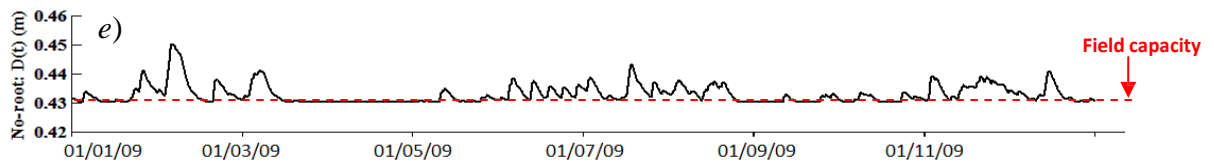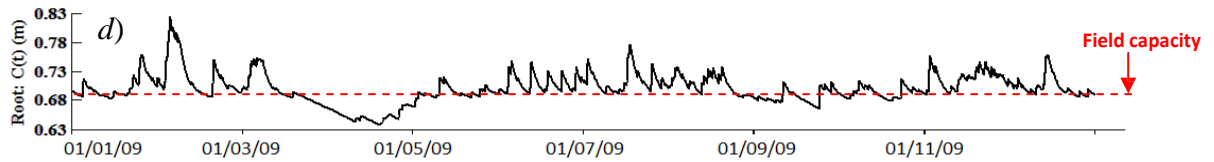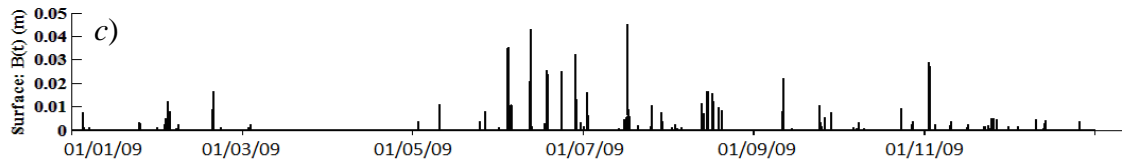
Figure 7. Model results: *a)* measured vs. modelled streamflow, *b)* modelled streamflow components. Water level in the model reservoirs: *c)* surface reservoir, *d)* non-saturated root reservoir (offset by $\theta_r\ C_H$ to show the absolute water content in the soil layer), *e)* non-saturated non-root reservoir (offset by $\theta_r\ D_H$) and *f)* aquifer reservoir.

48

a)

b)

57

58

c)

59

60
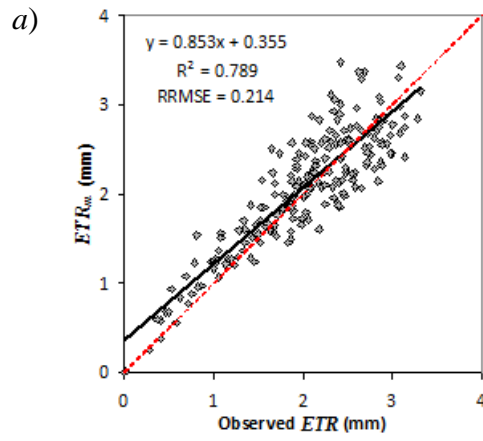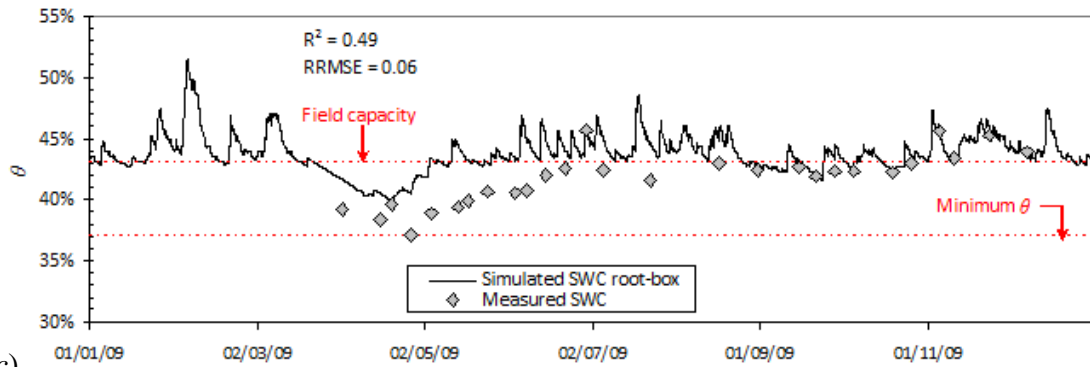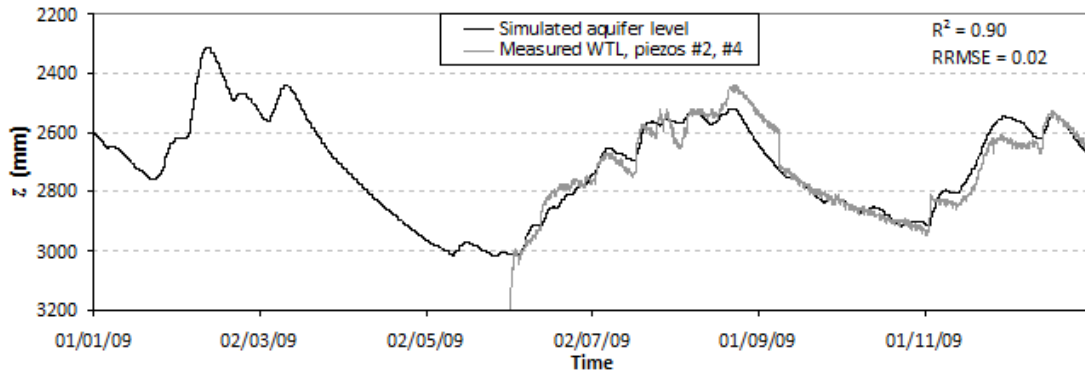
Figure 8. Validation of: *a*) daily evapotranspiration ETR_m, *b*) soil water content θ at the 1.6 m
root-reservoir and *c*) water table level *z*. (R^2: determination coefficient, RRMSE: relative root
mean squared error).

49
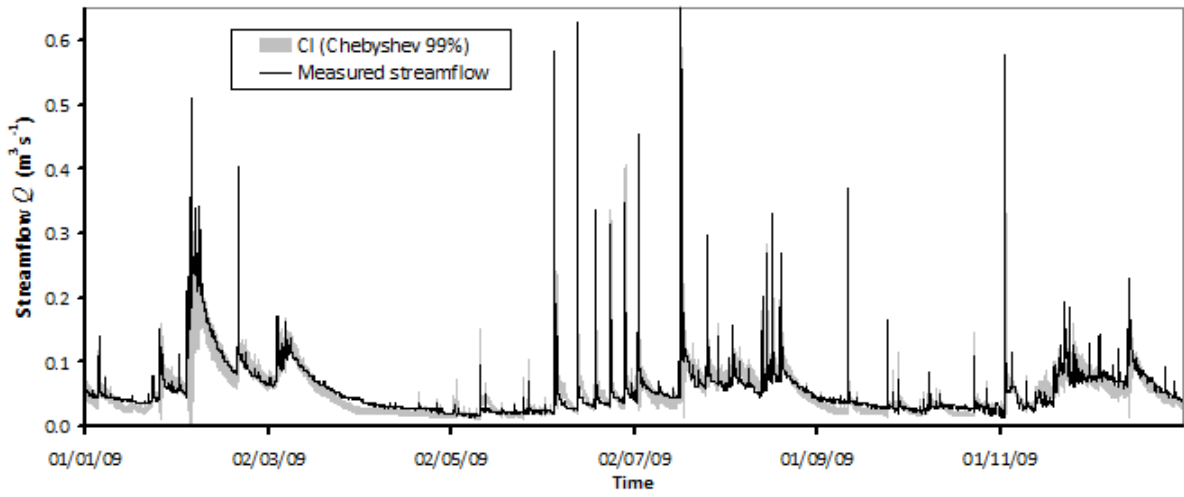
64

65

66   Figure 9. Measured streamflow against modelled 99% Chebyshev confidence interval

67   (vertical axis truncated at 0.6 m³ s⁻¹).
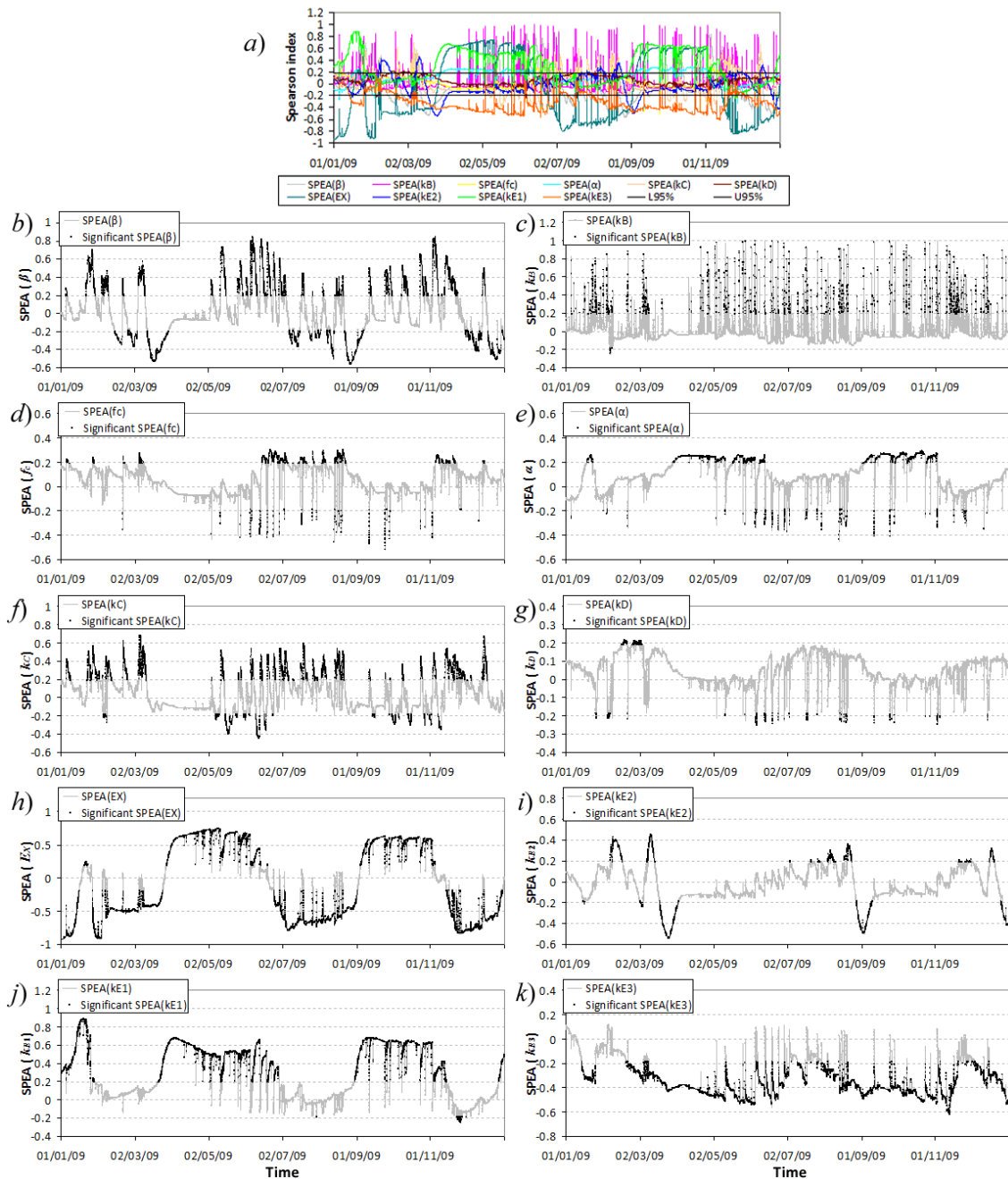
Figure 10. Spearman indexes between *Q* and: *a)* all the parameters: black horizontal lines indicate the 95% confidence interval out of which the Spearman is significant, *b)* partition parameter β , *c)* surface discharge k_B, *d)* infiltration rate at field capacity *fc*, *e)* maximum infiltration *α*, *f)* root-reservoir discharge *α*, *f)* root-reservoir discharge k_C, *g)* non-root discharge k_D, *h)* threshold for shallow aquifer E_X, *i)* shallow aquifer discharge k_{E2}, *j)* deep aquifer discharge k_{E1} and *k)* deep percolation discharge k_{E3}. The black dots indicate the time steps for which the Spearman is significant at the 95% confidence level, while grey dots indicate non-significant correlations.